Progress in Polymer Science 38 (2013) 1909–1928

Contents lists available at ScienceDirect

Progress in Polymer Science

journal homepage: www.elsevier.com/locate/ppolysci

Review

Recent trends in polymer tandem solar cells research

Jingbi You[a], Letian Dou[a], Ziruo Hong[c], Gang Li[a,*], Yang Yang[a,b,*]

[a] Department of Materials Science and Engineering, University of California, Los Angeles, CA 90095, USA
[b] California NanoSystems Institute, University of California, Los Angeles, CA 90095, USA
[c] The Research Center for Organic Electronics, Engineering School, Yamagata University, Yonezawa-shi, Yamagata 992-8510, Japan

ARTICLE INFO

Article history:
Received 20 October 2012
Received in revised form 16 April 2013
Accepted 20 April 2013
Available online 28 April 2013

Keywords:
Polymer solar cells
Multi-junction solar cells
Tandem structure
Polymers

ABSTRACT

Polymer solar cells have many intrinsic advantages, such as their light weight, flexibility, and low material and manufacturing costs. Recently, polymer tandem solar cells have attracted significant attention due to their potential to achieve higher performance than single cells. This trend article intends to provide the latest progress in polymer tandem solar cell technology with a focus on active layer materials and interfacial materials for sub-cell interconnection. Following an introduction of the structure and current status of polymer tandem solar cells, this article will review polymers which have been, and could be used, for tandem solar cells. Furthermore, this article will discuss the interconnecting layer consisting of p- and n-type interfacial layers, which is equally critical for polymer tandem solar cells. Finally, because tandem solar cell measurements are more complicated than that of single solar cells, this article will also address polymer tandem solar cell measurement issues.

Published by Elsevier Ltd.

Contents

1. Introduction 1910
2. Polymer tandem solar cells 1910
   2.1. Polymer tandem solar cells structure and operation mechanism 1911
   2.2. Development and current status of polymer tandem solar cells 1911
3. Polymer materials for tandem solar cells 1912
   3.1. Wide band gap polymers 1913
      3.1.1. Regioregular poly(3-hexylthiophene) (RR-P3HT) 1914
      3.1.2. Wide band gap polymers with a deep HOMO level 1914
   3.2. Low band gap (LBG) polymers 1915
      3.2.1. Polymers with band gap around 1.4 eV 1916
      3.2.2. Polymers with a band gap less than 1.3 eV 1920
   3.3. Medium band gap polymers (E_g ~1.6 eV) 1920
4. Tandem device engineering and measurement 1921
   4.1. Interconnecting layer for polymer tandem solar cells 1921
   4.2. Tandem solar cells measurement 1922
5. Conclusion and perspective 1923

* Corresponding authors at: Department of Materials Science and Engineering and California NanoSystems Institute, University of California, Los Angeles, CA 90095, USA. Tel.: +1 310 825 4052; fax: +1 310 206 7353.
E-mail addresses: gangl@ucla.edu (G. Li), yangy@ucla.edu (Y. Yang).

0079-6700/$ – see front matter. Published by Elsevier Ltd.
http://dx.doi.org/10.1016/j.progpolymsci.2013.04.005

6. Supplementary 1923
Acknowledgements 1925
References 1925

1. Introduction

Ever-increasing world energy demand, depletion of non-renewable energy resources and disruptive climate change due to greenhouse gases has aroused much interest in alternative renewable energy sources. Solar energy is the best of the available alternatives, for it is both abundant and clean. Discovery of the photovoltaic effect in silicon (Si) diodes in 1954 marked the dawn of the era of modern solid-state photovoltaic (PV) technology [1]. Currently, crystalline Si and various inorganic thin film solar cells are the dominant photovoltaic technologies. However, the cost of inorganic solar cells limits their wide acceptance and hence solar PV accounts for less than 0.1% of US energy generation. Intensive research has been conducted to develop low-cost PV technologies, and organic photovoltaics (OPVs) may be one of the most promising solutions [2–12]. Significant progress in bulk hetero-junction (BHJ) polymer solar cell technology has been achieved in the last decade. In particular, single junction cell efficiency has been doubled from 4% in 2005 [13,14] to 8–9% with the state-of-art cells [15–18]. Although technically impressive, it is not sufficient to allow direct competition against mature PV technologies. Several groups have predicted that the power conversion efficiency (PCE) limitation of single junction organic solar cells is ~10–12%, through optimization of materials with appropriate band gap, energy levels, and carrier mobility [19,20]. To achieve high power conversion efficiency, a balanced consideration of photocurrent, photovoltage and fill-factor needs to be implemented. Large photocurrent requires lower band gap material for more solar radiation harvesting, but this also means lower photovoltage. Charge carriers in organic semiconductors are transported via a hopping process, as organic molecules are bonded by weak intermolecular van de Waals interactions rather than covalent bonds in crystalline inorganic semiconductors. Therefore low carrier mobility (typically 10^{-7} to 10^{-3} cm^2/v.s. OPV materials) is an inherent limitation of organic materials. Although the absorption coefficients of organic semiconductors are high, low carrier mobility restricts the film thickness and this leads to insufficient photon absorption [2–12].

A major loss mechanism for single junction solar cells is the photovoltage loss due to the thermalization of hot carriers created when photons of energy greater than the band gap (which determines the photovoltage) are absorbed. The limitations of single junction photovoltaics can be overcome using tandem solar cells, in which two or more single cells absorbing complementary wavelength ranges are stacked together [21–23]. In this way, the photon utilization efficiency can be significantly improved and thermalization losses are lowered due to the use of materials having different band gaps. While the Shockley–Quiesser limitation of single junction solar cell is 33.7% at E_g ~1.4 eV [24], inorganic multi-junction solar cells with efficiency up to 43.5% have been achieved [25].

Brabec et al. predicted that 15% efficiency polymer tandem solar cells can be achieved in a two cell tandem configuration [26]. The simulations are based on the assumption of a constant (65%) external quantum efficiency (EQE) for both cells within the absorbed spectral range, i.e., both cells have a flat EQE from violet to their absorption edge. In reality, it is beneficial in the tandem approach to have two sub-cells with less overlap in absorption, as this can simplify the optimization process of the tandem structure. In tandem polymer solar cell design, this can be realized by selectively employing $PC_{61}BM$ or $PC_{71}BM$, which possess significantly different extinction coefficient due to their different molecular structure symmetry [27]. Yang et al. and Brabec et al. published excellent review articles on organic tandem solar cell providing comprehensive reviews of the different device structures and tandem cell working mechanisms [21,23]. The focus of this tandem polymer solar cell review is on the materials issues, both active layer materials and interfacial materials for sub-cell interconnection. The latest progress in polymer tandem solar cells and their performance measurement will also be included.

The outline of this review is as follows: the structure of tandem polymer solar cells and their development will be presented first followed by a review of the key components of high performance tandem solar cell wide (E_g > 1.7 eV) and low band gap polymers, and discussion of their application in tandem structures. The band gap polymers of interest will be divided into three categories: medium band gap polymers (~1.6 eV), low band gap polymers (~1.4 eV), and ultra-low band gap polymers (<1.3 eV). In addition to the photoactive layer materials, interconnecting layers connecting each sub-cell will be briefly discussed in this review with reference to their optical, mechanical and electrical requirements. Finally, efficiency measurement of tandem solar cells is not a trivial, and the measurement issue will be addressed.

2. Polymer tandem solar cells

Application of the tandem structure in organic solar cells began with small molecule fabricated through thermal evaporation. The vacuum evaporation process supports multilayer structures of organic small molecule light emitting diodes (OLEDs) and OPVs, which naturally can be extended into tandem structures by evaporating more layers. In 2002, Forrest et al. showed that an ultrathin evaporated metal between two sub-cells can lead to the addition of their photovoltages [28]. Currently, Heliotek and Leo's group in Institut für Angewandte Photophysik (IAPP) in Germany are the technical leaders in small molecule tandem OPV [29,30].

List of symbols

BDT	benzodithiophene
BDTT	thienyl benzodithiophene
BHJ	bulk hetero-junction
BT	benzothiadiazole
CB	chlorobenzene
CPDT	cyclopentadithiophene
DMF	dimethylformamide
DTG	dithieno[3,2-b:2′,3′-d] germole
DTS	dithieno[3,2-b:2′,3′-d] silole
DPP	diketopyrrolopyrrole
EQE	external quantum efficiency
E_g	optical band gap
FF	fill factor
HOMO	highest occupied molecular orbital
ICL	interconnecting layer
$IC_{60}BA$	indene-C60 bisadduct
IQE	internal quantum efficiency
J_{SC}	short circuit current
LBG	low band gap polymer
LUMO	lowest unoccupied molecular orbital
MBG	medium band gap
NREL	National Renewable Energy Laboratory
ODCB	1,2-dichlorobenzene
OPV	organic photovoltaics
OSMSS	one-sun multi-source simulator
PCE	power conversion efficiency
$PC_{61}BM$	[6,6]-phenyl-C61-butyric acid methyl ester
$PC_{71}BM$	[6,6]-phenyl-C71-butyric acid methyl ester
P3HT	poly(3-hexylthiophene)
PCPDTBT	poly[2,6-(4,4-bis-(2-ethylhexyl)-4H-cyclopenta[2,1-b;3,4-b′] dithiophene)-alt-4,7-(2,1,3-benzothiadiazole)]
PBDTT-DPP	poly{2,6′-4,8-di(5-ethylhexylthienyl)benzo[1,2-b;3,4-b]dithiophene-alt-5-dibutyloctyl-3,6-bis(5-bromothiophen-2-yl)pyrrolo[3,4-c]pyrrole-1,4-dione}
PDTP-DFBT	poly[2,7-(5,5-bis-(3,7-dimethyloctyl)-5H-dithieno[3,2-b:2′,3′-d]pyran)-alt-4,7-(5,6-difluoro-2,1,3-benzothia diazole)]
PMDPP3T	poly[[2,5-bis(2-hexyldecyl-2,3,5,6-tetrahydro-3,6-dioxopyrrolo[3,4-c]pyrrole-1,4-diyl]-alt-[3′,3″-dimethyl-2,2′:5′,2″-terthiophene]-5,5″-diyl]
PSCs	polymer solar cells
PT	thiadiazolo[3,4-c]pyridine
TAZ	benzotriazole
TPD	thieno[3,4-c]pyrrole-4,6-dione
TT	thienothiophene
ULBG	ultra-low band gap
V_{OC}	open circuit voltage
WBG	wide bandgap polymer

Compared to cells prepared by evaporation of small molecule cells, polymer solar cells have better device performance and simplified device structure in single-junction devices. The polymer tandem concept was introduced later mainly due to the lack of good solution processed interconnecting layers. The advantages in cost saving, along with the fast advances in active materials and interfacial layers in single junction polymer solar cells, have accelerated significant research efforts in polymer tandem solar cell. A 10.6% power conversion efficiency in a polymer tandem solar cell has now been achieved [31].

2.1. Polymer tandem solar cells structure and operation mechanism

Fig. 1(a) depicts a typical polymer tandem cell comprising wide band gap and low band gap polymer solar cells, with an interconnecting layer (ICL). Each cell is a donor–acceptor (D–A) bulk hetero-junction solar cell. Fig. 1(b) shows the solar spectrum, the absorption of wide and low band gap cells. When stacking two complementary cells with a large (E_g ~1.9 eV) and small band gap (E_g ~1.4 eV) polymer, 60% of the photons from the sun can be covered [21]. The two sub-cells in the tandem device may be connected either in series [22] or in parallel [23] by varying the interconnecting scheme. The series connection is the most widely adopted one, and the energetic diagram of the device can be represented as in Fig. 2 [26]. Here, we define the sub-cell close to glass/ITO substrate side as front cell, and the sub-cell far away from glass/ITO substrates as rear cell. To maximize utilization of higher energy photons and to improve current balance, the wide and low band gap polymer based sub-cells are usually used as front and rear cell, respectively [23]. The function of the interconnecting layer is to ensure the alignment of the quasi-Fermi level of electrons in the acceptor of the front cell with the quasi-Fermi level of holes in the donor of the rear cell (or vice versa in an inverted architecture). In other words, the intermediate layer should allow the recombination of holes coming from one sub-cell with electrons coming from the other, and the open circuit voltage of the tandem solar cell will be the sum of the two sub-cells.

2.2. Development and current status of polymer tandem solar cells

To construct high efficiency tandem polymer solar cells, high performance individual cell using polymers with complementary absorption are needed. In the early years of polymer solar cells development, the demonstration of the tandem polymer solar cell concept were first conducted based on the V_{OC} addition using two photovoltaic cells that were fabricated from the same conjugated polymer (PPV derivative or P3HT) [32–34] or polymer/small molecule hybrid [35–37]. Yang et al. first demonstrated a semi-transparent version of MEH-PPV based polymer solar cell, and stacked it directly with another non-transparent solar cell to realize the concept [32]. In such a stacked geometry with identical absorption spectra, the thickness of the organic films is the major parameter to tune the relative performance of the two cells to realize an optimal tandem

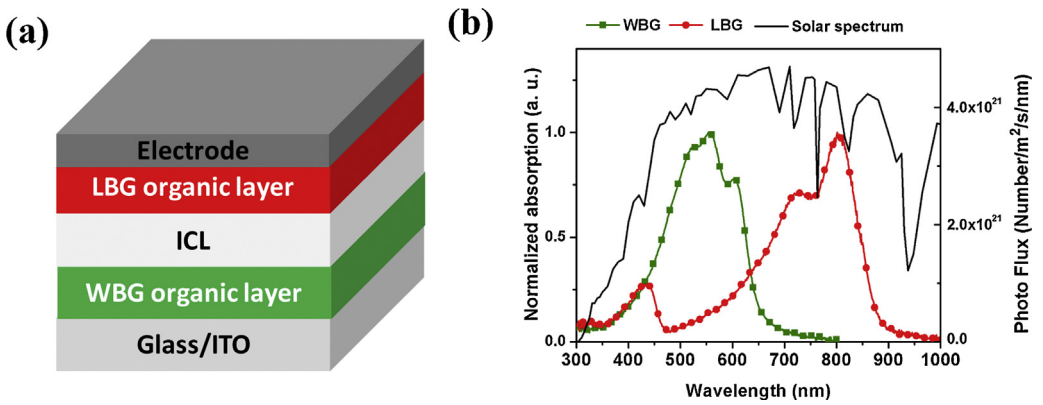

Fig. 1. (a) Tandem polymer device structure including wide bandgap polymer solar cell (front cell), and low bandgap polymer solar cell (rear cell), front and rear cells are connected to each other by an interconnecting layer (ICL), and (b) typical wide band gap polymer (green), low bandgap polymer (red) absorption and solar spectrum. (For interpretation of the references to color in this figure legend, the reader is referred to the web version of the article.)

cell. The first polymer tandem solar cell consisting of two sub-cells with different materials was demonstrated in 2006 by Boer and Janssen et al. [38]. The absorption spectra and tandem device structure are shown in Fig. 3. Even though the tandem efficiency is only about 0.57%, the efficiency has been greatly improved compared with the each sub-cell. In 2007, Kim et al. used the (n-type) TiO_2/(p-type) PEDOT:PSS interconnecting layer to bridge two higher performance single cells to realize a tandem structure [39]. The front cell active layer is poly[2,6-(4,4-bis-(2-ethylhexyl)-4H-cyclopenta[2,1-b;3,4-b′] dithiophene)-alt-4,7-(2,1,3-benzothiadiazole)] (PCPDTBT) and [6,6]-phenyl-C61 butyric acid methyl ester (PCBM) blend, and the rear cell is made of poly(3-hexylthiophene) (P3HT) and [6,6]-phenyl-C71 butyric acid methyl ester ($PC_{71}BM$). With the front and rear cell of 3.0 and 4.7% efficiency, respectively, a 6.5% efficiency of tandem solar cell was achieved. The low band gap polymer PCPDTBT cell showed lower quantum efficiency and fill factor (FF) than the P3HT:PCBM cell and this limited the performance of the tandem device. Yang et al. recently designed a special low band gap polymer poly{2,6′-4,8-di(5-ethylhexylthienyl) benzo[1,2-b;3,4-b]dithiophene-alt-5-dibutyloctyl-3,6-bis (5-bromothiophen-2-yl)pyrrolo[3,4-c]pyrrole-1,4-dione} (PBDTT-DPP) with band gap of ~1.45 eV. This material is specially designed with narrow absorption to avoid the overlap with wide band gap polymer P3HT. Regular and inverted structure single junction devices both showed 6–7% efficiency with fill factor close to 70%. This forms an excellent combination with a P3HT:ICBA cell as the wide band gap cell resulting in a tandem efficiency of 8.62% (certified by NREL) [40]. This new concept represented a breakthrough in polymer tandem solar cells. The device structure and the certified results are shown in Fig. 4. Further improvement in material and processing has led to a 10.6% PCE efficient tandem solar cell [31]. This paves a solid ground for targeting 15% PCE in the near future. In the following sections, we will concentrate on the polymer materials, including the polymers, which have been or could be used for tandem polymer solar cells, and also we will discuss the interconnecting layers' materials.

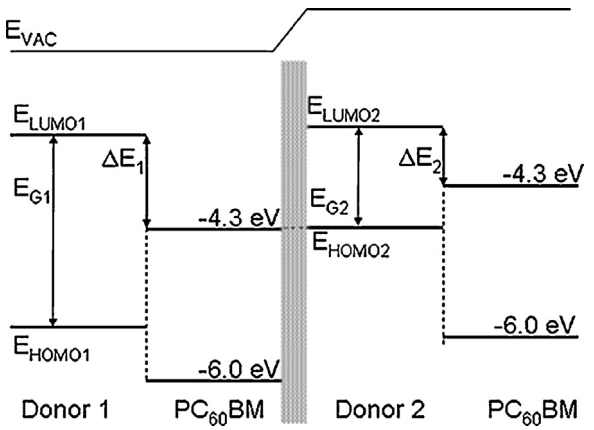

Fig. 2. The band alignment of a tandem polymer solar cell contains two junctions, where $PC_{60}BM$ is assumed to the acceptor material for each cell [26].
Copyright 2008. Reproduced with permission from Wiley-VCH.

3. Polymer materials for tandem solar cells

The simplest form of a multi-junction solar cells – the double junction tandem solar cells, consists of a front cell with a wide band gap and a rear cell with a low band gap, or vice versa. The polymer band gap for each sub-cell should be selected carefully to achieve high performance tandem solar cells. Brabec et al.'s simulation showed that to achieve 15% efficiency in a tandem solar cell, the WBG cell donor should have a band gap of 1.6 eV, and the LBG cell donor should have a band gap of 1.3 eV, under the assumption that both cells have a flat quantum efficiency of 65% (see Fig. 5) [26]. In reality, the external quantum efficiency of the low band gap (<1.5 eV) polymer solar cell is typically less than 50% [41–43]. In this review, we will mostly focus on wide band gap polymers with around 1.9 eV as front cell materials as poly(3-hexylthiophene) (P3HT, E_g = 1.9 eV) is so far the most successfully used WBG polymer in tandem polymer solar cell.

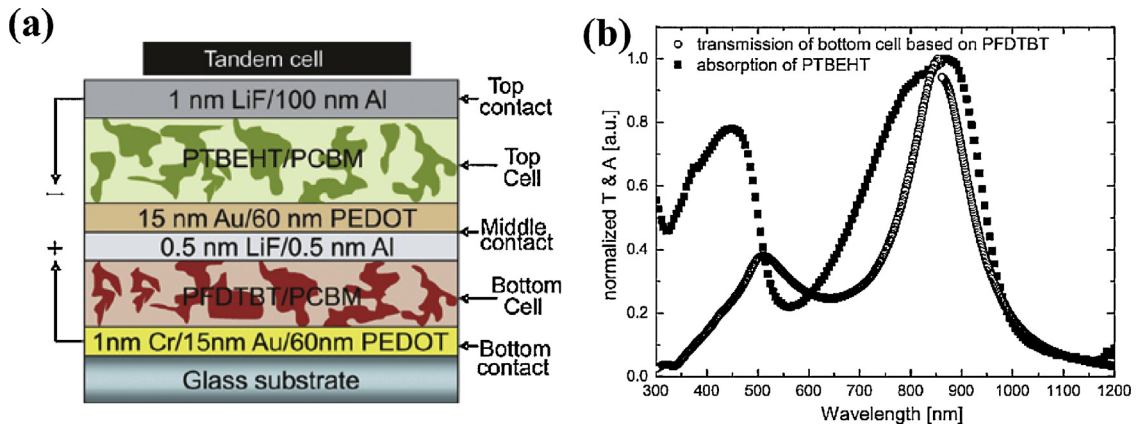

Fig. 3. (a) First polymer tandem cell using a combination of low band gap polymer (PTBEHT) and a large band gap polymer (PFDTBT) system fabricated by Hadipour et al. (b) The light output of the bottom cell consisting of glass/1 nm Cr/15 nm Au/60 nm PEDOT:PSS/110 nm PFDTBT:PCBM (1:4)/0.5 nm LiF/0.5 nm Al/15 nm Au (circles) and the absorption of the small-bandgap polymer (PTBEHT) of the top cell [38].

In polymer solar cell research, the term low band gap polymer (LBG) is loosely defined and changes with time. Polymers with smaller band gaps than P3HT are typically called LBG polymers now, but even P3HT was called LBG when MEH-PPV is the champion. In tandem application, a polymer with a band gap above 1.7 eV is inappropriate to be used for the tandem solar cell as a LBG cell because it would have too much overlap with the WBG cell. In this tandem solar cell review, we divide polymers with band gaps over 1.7 eV wide band gap (WBG) polymers, and those with band gaps less than 1.5 eV are classified as low band gap (LBG) polymers. For polymers with a band gap between 1.5 and 1.7 eV, they could serve in both roles, and we will call them medium band gap (MBG) polymers. Based on these clearly defined categories, we will review the recent polymer materials that have been used and could be used for tandem solar cells. We will discuss these materials based on several key factors, including absorption, energy alignment, solubility, morphology and mobility.

3.1. Wide band gap polymers

One of the earliest polymer for solar cell is the wide band gap poly[2-methoxy,5-(2′-ethyl-hexyloxy)-p-phenylenevinylene] (**MEH-PPV**) developed by Wudl et al. [44]. A higher PCE of >3.0% was achieved for PPV-based PSCs [27] when combined with an acceptor which gave higher absorption. However, further improvement in MEH-PPV system was limited due to its relatively low hole mobility and narrow light absorption range. Benefitting from the higher hole mobility [13] and broader spectrum coverage, in soluble polythiophene systems (e.g. **P3HT**), the maximum external quantum efficiency (EQE) can reach over 70%. The short current is typically about 10 mA/cm^2

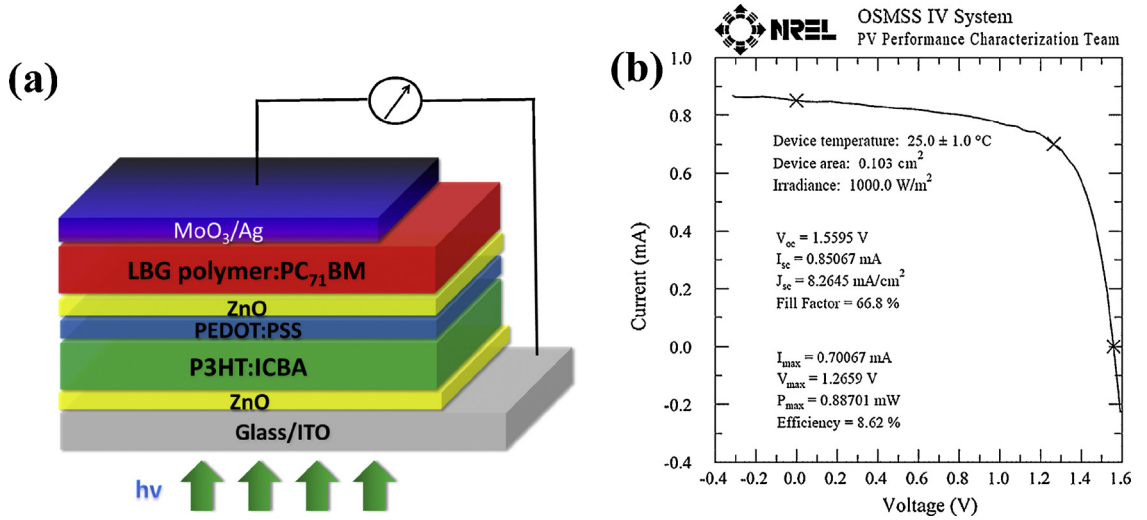

Fig. 4. (a) The structure of a high performance inverted tandem solar cell using wide and low bandgap polymers as front and rear cells, respectively, and (b) The *J*–*V* curve of inverted tandem cell as certified by National Renewable Energy Laboratory (NREL) [40].

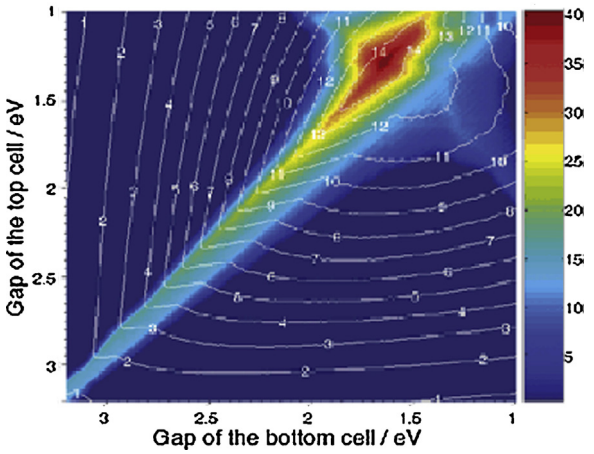

Fig. 5. Percentage of efficiency increase of a tandem cell over the best single cell (R) for a device comprising a top sub-cell and a bottom sub-cell based on donors having a LUMO level at –4 eV. The variables are the band gap of both donors. The lines indicate the efficiency of the tandem devices [26].

[13]. Although not a champion in single junction solar cells anymore, P3HT is so far the most studied and successful wide band gap polymer in polymer tandem solar cells.

3.1.1. Regioregular poly(3-hexylthiophene) (RR-P3HT)

Regioregular poly(3-hexylthiophene) (RR-P3HT) was invented in the early 1990s [45,46] and is a large band gap polymer with a band gap of (1.9 eV).The chemical structure is shown in Fig. 6. The absorption covers the visible region with cut off at 650 nm. The self-organization of the polymer leads to high mobility (up to 0.1 $cm^2 V^{-1} s^{-1}$ in a π–π stacked transistor configuration [47], and $\sim 10^{-4}$ in a PV configuration [13]), and relatively high performance solar cells based on P3HT:PCBM have been achieved in 2005 through various morphology control approaches [13,14]. The improvement in buffer layer led to about 5.2% efficiency by using NiO_x to replace PEDOT:PSS [48]. In previous work, the P3HT:PCBM system was successfully used as a front cell for tandem solar cell. The short circuit current of that cell was about 7.4 mA/cm^2, which was limited by the rear cell, and 5.8% PCE was achieved [49]. The limited J_{SC} is due to the material limitation of the rear cell. Despite the high mobility and good phase separation of the P3HT:PCBM blend, the V_{OC} generated by such a large band-gap (1.9 eV) cell is only 0.6 V, indicating a photon energy loss of over 70%. Thus, enhancing the V_{OC} of front cell become important and it will directly improve the overall tandem solar cell performance accordingly. This has been achieved by lifting up the LUMO of the acceptor. Recently, the V_{OC} of the P3HT system has been significantly improved from 0.60 to 0.84 V by using new fullerene derivative indene-C_{60}-bisadduct ($IC_{60}BA$), which has a higher LUMO level [50,51]. By replacing P3HT:PCBM with P3HT:ICBA as a front cell for tandem cells, the efficiency of the tandem cell has been increased from 5.8% to 7%, mainly due to the V_{OC} improvement from 1.3 V to 1.56 V [49,52]. The chemical structures of P3HT, $PC_{61}BM$, $PC_{71}BM$ and ICBA are shown in Fig. 6.

3.1.2. Wide band gap polymers with a deep HOMO level

In addition to lifting up the LUMO of the fullerene by using strong electron donating groups to enhance open circuit voltage, lowering the HOMO of the donor material by using less electron-deficient groups is an equivalent approach.

Thiophene is an electron-rich group [53,54] and the HOMO level of P3HT is about −5.0 eV. Therefore, the V_{OC} of the P3HT:PCBM is restricted. By utilizing less electron-rich and strongly electron-deficient groups, the HOMO level can be effectively lowered. For example, fluorene, carbazole and benzodithiophene (BDT) units are commonly used in wide band gap materials because they are less electron rich. Benzothiadiazole (BT), benzotriazole (TAZ) and thieno[3,4-*c*]pyrrole-4,6-dione (TPD) units are popular due to their strong electron-deficiency [55–64]. In 2004, Cao et al. demonstrated a polymer containing alternating carbazole and thiophene-BT-thiophene units that achieved a V_{OC} of 0.95 V, however, the single cell device showed only 2.24% efficiency [55]. Recently, high performance wide band gap polymers (**P1**–**P7**) have been reported [56–64]. In 2006, Janssen et al. synthesized a donor material poly[2,7-(9,9-didecylfluorene)-alt-5,5-(4′,7′-di-2-thienyl-2′,1′,3′-benzothiadiazole)] (**P1**) with a band gap of 1.9 eV. The very low HOMO of this wide band gap polymer leads to a much higher V_{OC} of 0.98 V in **P1**:PCBM solar cells. Later, **P1** was applied in tandem solar cells by the same group and a V_{OC} as high as 1.58 V was achieved. Unfortunately, the low EQE of the front and rear cell limited the tandem devices to only 4.9% in efficiency [56]. Based on the similar chemical structure as **P1**, Leclerc and Heeger et al. synthesized WBG polymer (**P2**), and used a thin TiO_x layer as an optical spacer, they showed the internal quantum efficiency (IQE) of a single cell device can achieve almost 100% and thus a high PCE of 6% was obtained [57]. Recently, Yang et al. reported a wide band gap polymer based on BDT and thiophene-BT-thiophene units (**P3**) and You et al. reported a polymer based on BDT and thiophene-TAZ-thiophene units (**P4**). These polymers showed similarly high V_{OC} and PCE [58,59]. Several other wide band gap polymers also showing higher V_{OC} and higher efficiencies in single junction cells. For example, TPD-based polymers (**P5**) showed a V_{OC} of about 0.85 V, and short currents close to 10 mA/cm^2. The TPD based materials also showed encouraging charge transport properties [60–62]. As a result, the power conversion efficiency is over 6%. Based on the promising electronic properties of the TPD unit, Tao et al. developed a polymer family based on TPD and dithieno[3,2-b:2′,3′-d]silole (DTS), and Reynolds et al. developed a family based on TPD and dithieno[3,2-b:2′,3′-d] germole (DTG) alternating units. The band gaps for **P6** [63] and **P7** [64] were around 1.7 eV. Their low-lying HOMO levels ($\sim$−5.5 eV) suggest that a high V_{OC} should be obtainable. Together with the high hole mobilities, the **P6** polymer reached a PCE of 7.3%, with V_{OC} = 0.88 V, J_{SC} = 12.2 mA/cm^2, and FF = 0.68; whereas **P7** reached 7.3% PCE with V_{OC} = 0.85 V, J_{SC} = 12.6 mA/cm^2, and FF = 0.68.

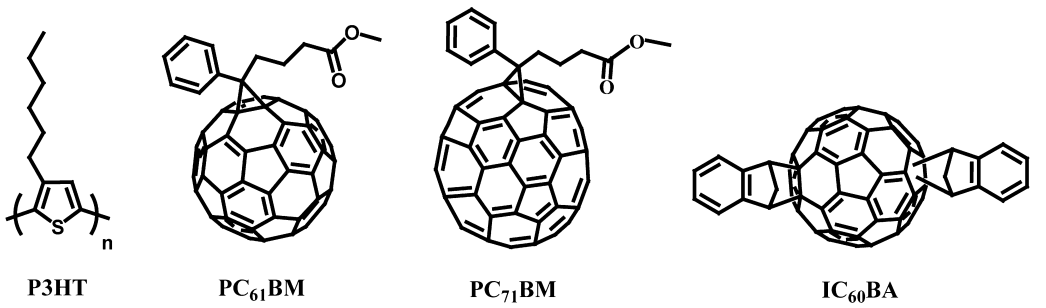

Fig. 6. The chemical structure of P3HT, $PC_{61}BM$, $PC_{71}BM$ and $IC_{60}BA$.

The chemical structures of these polymers are drawn in Fig. 7, and the performance parameters of these materials are summarized in Table 1. Although it has not been tried yet, high performance tandem polymer solar cells based on these WBG polymer in the front cell could be achieved in the near future due to their promising features.

3.2. Low band gap (LBG) polymers

To achieve high efficiency tandem polymer solar cells, it is essential to have a high performance low band gap polymer for the rear cell to match the current of the front cell. Because the two sub-cells are connected in series, the overall current of the tandem device will be

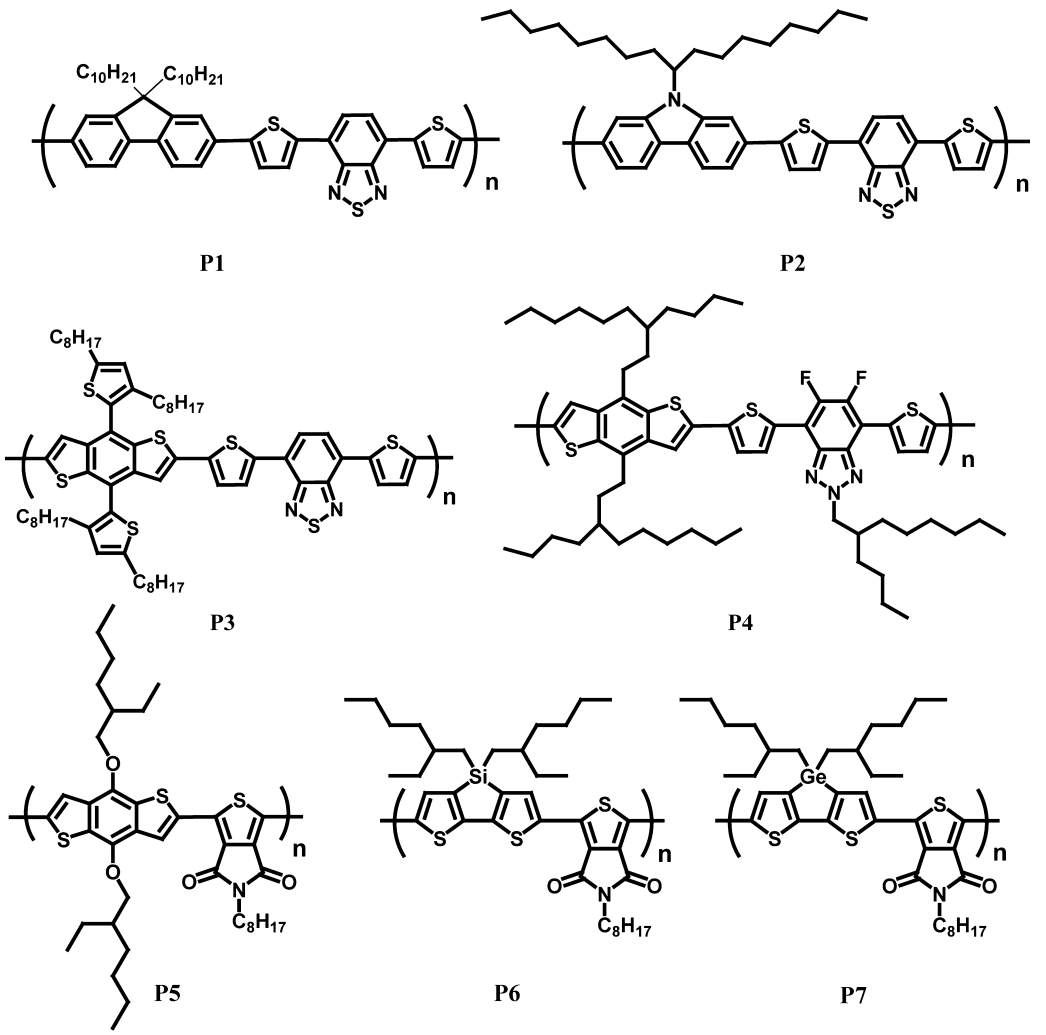

Fig. 7. The chemical structures of high performance wide bandgap polymers (**P1**–**P7**) with deep LUMO levels.

Table 1
The parameters of high performance wide bandgap polymer solar cells.

Active layer	Bandgap (eV)	HOMO (eV)	V_{OC} (V)	J_{SC} (mA/cm^2)	FF (%)	PCE (%)	References
P3HT:PC_{60}BM	1.90	−5.0	0.6	10	70	4.2	[13,14]
P3HT:ICBA	1.90	−5.0	0.84	10.6	72.7	6.5	[50,51]
P1	1.95	~−5.5	0.98	5.5	52	2.8	[56]
P2	1.90	−5.5	0.88	10.6	66	6.1	[57]
P3	1.8	−5.3	0.92	10.7	57.5	5.7	[58]
P4	2.0	−5.36	0.79	11.8	73	7.1	[59]
P5	1.8	−5.4	0.85	11.6	68	6.6	[60–62]
P6	1.73	−5.57	0.88	12.2	68	7.3	[63]
P7	1.69	−5.65	0.85	12.6	68	7.3	[64]

limited by the sub-cell with lower current. Thus, the most important criterion for the rear cell polymer is current matching, which means that it can provide a same photocurrent as the front cell when applied into the tandem structure. Assuming the front cell polymer has a band gap around 1.9 eV, it is necessary for the rear cell polymer to have a band gap sufficiently lower to harvest the light that passes through the front cell. Currently, there are intensive studies on design and synthesis of new LBG polymers for photovoltaic applications. By using the electron push–pull strategy and the stabilization of the quinoid resonance structure approach, band gap as low as 1 eV can be easily obtained [65]. However, high photovoltaic performance requires a comprehensive consideration, far beyond the low band gap only. High hole mobility of the polymer is required to support efficient charge transport; the polymer should also have proper HOMO/LUMO levels to (a) maximize V_{OC} and (b) maintain a large enough offset (>0.3 eV) between polymer and acceptor's LUMO for efficient charge separation at the donor–acceptor interface. Finally, the active layer should form a bi-continuous interpenetrating network of both donor and acceptor with the dimension of each domain being around 20 nm (~twice the exciton diffusion length L_D). The morphology of the blend film is critically important due to the relatively short lifetime and low mobility of the excitons and charge carriers. These set stringent restrictions on promising candidates for polymer solar cells, particularly in tandem structures with more processing requirements. Among hundreds of LBG polymers reported in the last decade, only a small fraction of them satisfy the requirements well and show potential in polymer tandem solar cells. In retrospect, we look at the LBG polymers that have been used in tandem PSCs and also discuss the potential application of some of the latest LBG polymers in tandem structures in terms of current matching. We assume the band gap of the WBG cell polymer is 1.9 eV (absorption onset ~650 nm) and the WBG cell photo-current is 10 mA/cm^2 (EQE ~65%) under AM1.5G (1 sun) conditions. About 70% of the photons with energy higher than 1.9 eV will be absorbed by the WBG cell and EQE for the LBG cell between 300 nm and 650 nm is 20%. These are typical values in the state-of-art tandem polymer solar cells. Three groups of polymers (medium band gap, E_g ~1.6 eV; low band gap, E_g ~1.4 eV and ultra-low band gap, E_g < 1.3 eV) are discussed separately.

3.2.1. Polymers with band gap around 1.4 eV

Low bandgap polymers showing less absorption overlap with wide bandgap polymer will be more suitable for the tandem devices. In 2006, a promising LBG polymer **P8** (E_g = 1.4 eV) was reported by Brabec et al. at Konarka, with a PCE of 3.2% (Fig. 8) [66]. It is based on alternating strongly electron rich cyclopentadithiophene (CPDT) and strongly electron deficient benzothiadiazole (BT) units. Such a low band gap and decent performance were very encouraging at the early stage in the OPV field. In 2007, Bazan and Heeger et al. optimized the performances of solar cells by introducing solvent additives to improve the morphology. The optimized morphology led to significantly higher J_{SC} (16 mA/cm^2) and PCE of 5.5% [41,67]. The polymer blend absorbs from 350 nm all the way to nearly 900 nm with an average EQE value of ~45%, with 0.62 V V_{OC} and 55% FF achieved. Due to these advantages, Heeger et al. selected **P8** as the LBG cell in an all-solution processed tandem polymer solar cell, in which a combination of titanium oxide (TiO_x) and PEDOT:PSS layers were used as an interconnecting layer to connect the front cell and the rear cell [38]. The authors have chosen an unconventional structure with the low band gap BHJ composite (**P8**:PCBM) as the front cell and the wideband gap BHJ composite (P3HT:PC_{71}BM) as the rear cell. The maximum efficiency of 6.5% (J_{SC} = 7.8 mA/cm^2, V_{OC} = 1.24 V, FF = 0.67) was achieved in this study under an illumination of 100 mW/cm^2, based on a 3% efficiency front and a 4.7% efficiency rear cell. Later, Yang et al. reported a new LBG polymer poly[(4,4′-bis(2-ethylhexyl)dithieno[3,2-*b*:2′,3′-*d*]silole)-2,6-diyl-alt-(2,1,3-benzothiadiazole)-4,7-diyl] (**P9**, **PSBTBT**) replacing a carbon atom with a silicon atom as the bridging atom between the two thiophenes [42,68,69]. The optical band gap (1.45 eV) is very close to that of **P8**. It was found that the hole mobility of this polymer is 3×10^{-3} cm^2 V^{-1} s^{-1}, which is approximately three times higher than the mobility of **P8**. The V_{OC} of **P9** was slightly higher at 0.68 V but the J_{SC} was lower at 12.7 mA/cm^2 and that leads to a PCE of 5.1%. They also showed that the C—Si bond is longer than the C—C bond in the cyclopentadithiophene core. Consequently, there is less steric hindrance created by the dithienosilole core, leading to better π–π stacking [68]. They used **P9**:PC_{71}BM cell as the rear cell since the light intensity received by the rear sub-cell is attenuated by ~40% after passing through the front P3HT:PCBM sub-cell. The thickness of the rear

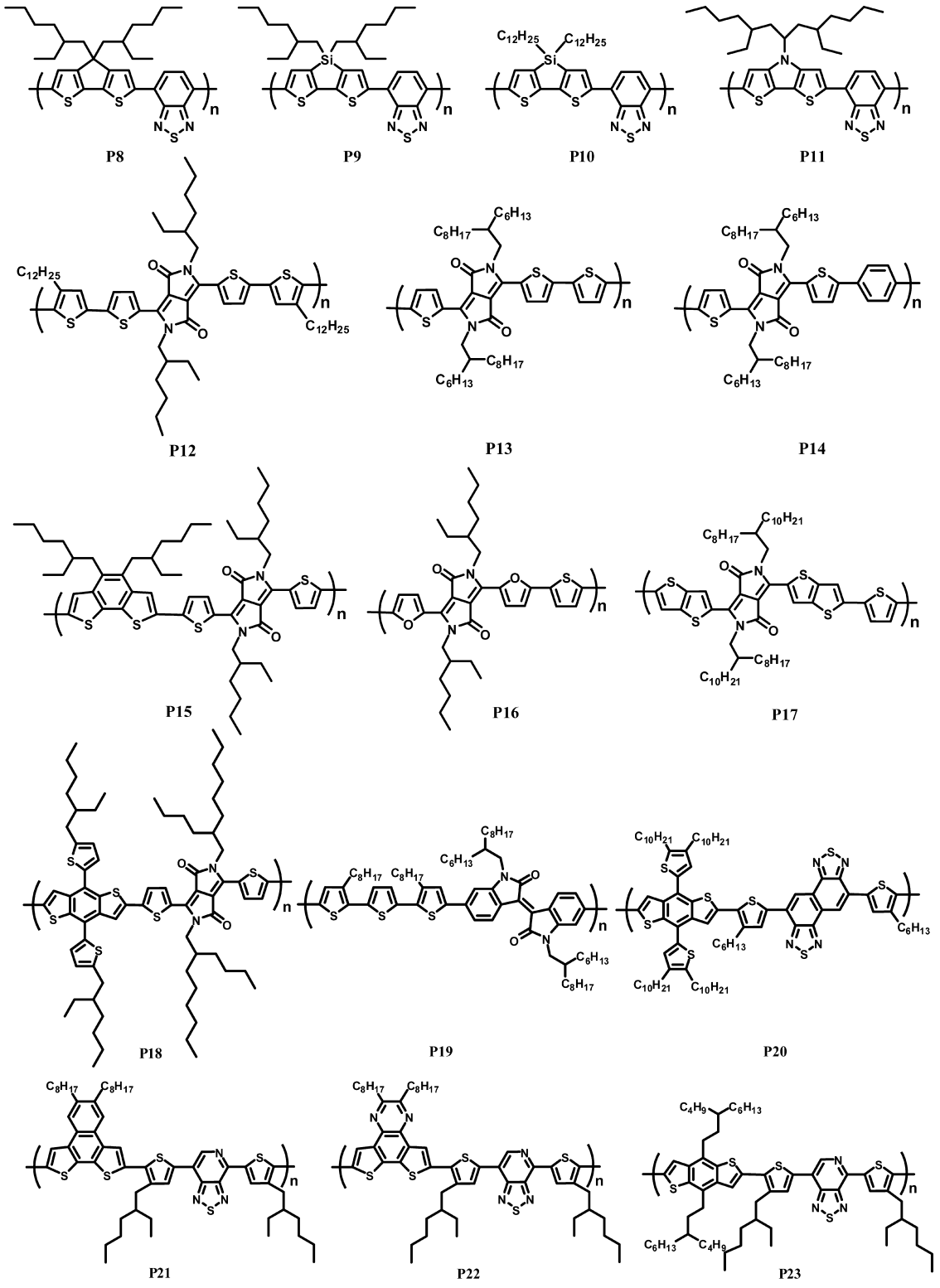

Fig. 8. The chemical structures of high performance low bandgap polymers (**P8**–**P23**) with bandgaps around 1.4 eV.

sub-cell using PSBTBT:$PC_{71}BM$ was unchanged, while photocurrent balance between the two sub-cells was achieved by varying the thickness of the front P3HT:PCBM cell. The combination of minimal absorption overlap between the PSBTBT and P3HT cells, the high FF, optimized optical field distribution, as well as a good interconnecting layer led to high performance tandem cells with PCE close to 6% [49]. Further optimization on this system was performed replacing PCBM with ICBA to improve theP3HT front cell V_{OC}. As the V_{OC} increased from 1.24 eV to 1.47 eV, the PCE was improved to 7% [52]. Bazan et al. reported even more impressive results with this particular polymer (**P10**, has different side chains than **P9**) in single junction devices [70], where they replaced the 2-ethylhexylchains on the silicon atom by long n-dodecyl side chains. **P10** was obtained by Stille coupling polymerization using a newly developed microwave-assisted method, which led to higher number average molecular weight of 44 kDa. The PCE of the devices based on this polymer were also higher, reaching a maximum of 5.9%, with an enhanced J_{SC} at ~17 mA/cm^2 [70]. Its application in tandem polymer solar cells seems to be promising. By further changing the silicon atom to a nitrogen atom, **P11** was synthesized by Wang et al. [71]. The 1-pentylhexyl side chain on the nitrogen atom gave the best results. A reasonable Mn of 18 kDa was obtained and the optical band gap was very similar to **P8** and **P9**. However, the HOMO and LUMO energy levels are much higher. This could cause some stability issues under ambient conditions and decrease the V_{OC} of the device significantly. The best solar cell that was fabricated with this material and PCBM (1:3) led to a PCE of 2.8%, mainly due to the low V_{OC} and FF value [71].

Another type of LBG polymers is based on the diketopyrrolopyrrole (DPP) unit, which was developed in the last 3–4 decades for high performance pigments. It is highly absorbing in the visible region and strongly electron withdrawing. When polymerized with electron donating monomers, the resulting polymers typically show energy band gaps smaller than 1.5 eV. Another attractive property is its good charge carrier mobility for both holes and electrons. In fact, one of the first organic electronic applications for DPP-based polymers was ambipolar organic thin film transistor (OTFT) [72].

In addition, the DPP core is particularly interesting for manufacturing considering due to its easy synthesis. The first highly performing polymer based on the DPP unit was reported by Janssen et al. in 2009 (Fig. 8), **P12** contains a backbone of alternating DPP and bithiophene units and has a small band gap of 1.4 eV [73]. Due to the poor solubility, it can only be fully dissolved in chloroform. The **P12**/PCBM film spin-cast from a chloroform solution showed amorphous polymer morphology due to the fast solvent evaporation, which suppresses polymer crystallinity and phase separation. Therefore, the cell only exhibited a very low EQE of 13% at 680 nm. It was found that by using a chloroform/ODCB mixture (4:1) to process the active layer, crystallinity can be significantly enhanced and the best device using **P12**/PCBM (1:2, w/w) gave a PCE of 3.2% [73]. By utilizing $PC_{71}BM$ as the acceptor, the photovoltaic performance was further improved to 4.0% with an FF of 0.58, a V_{OC} of 0.61 V, and a J_{SC} of 11.3 mA/cm^2 [73]. The authors also applied this material into a tandem device. They choose **P1** as the front (WBG) cell active material because of its proper band gap (1.9 eV) and low-lying HOMO level (-5.6 eV), which should lead to higher V_{OC} than traditional P3HT [56]. Due to the higher J_{SC} and lower FF of the front cell and lower J_{SC} and higher FF of the rear cell, optimizing the overall PCE become more complicated. A combined analysis of the optical absorption and electrical characteristics of individual single-junction sub-cells is shown to be essential to identify the optimum device layout of the corresponding tandem cell [74]. It is interesting that they found matching the photocurrents of the sub-cells is not a leading design criterion for optimum performance, because the short-circuit current of a polymer tandem cell can exceed that of the current-limiting sub-cell. A solution-processed polymer tandem cell with an efficiency of 4.9% (J_{SC} = 6.0 mA/cm^2, V_{OC} = 1.58 V, FF = 0.52) under AM1.5G 1-sun conditions has been obtained [56,74]. The EQE for the rear cell was however only around 35% from 650 nm to 800 nm. Due to the poor fill factor of the front cell, the total FF was limited to 0.52. By improving these two factors, higher overall PCE is expected.

Dozens of newly designed DPP based LBG polymers were reported since 2009; the high photovoltaic performance examples are shown in Fig. 8 (**P13**–**P18**). Janssen et al. reported that by co-polymerizing with a simple thiophene or benzene units, two new LBG polymers **P13** and **P14** were successfully synthesized [75,76]. **P13** shows a high molecular weight (54 kDa) and a very low band gap of 1.3 eV. High hole mobility of 1×10^{-2} cm^2 V^{-1} s^{-1} was achieved infield-effect transistors. This low band gap polymer showed a photo-response up to 900 nm when combined with $PC_{71}BM$, and EQE can reach around 35% in this region. High photovoltaic performance of 4.7% with J_{SC} = 11.7 mA/cm^2, V_{OC} = 0.65 V and FF = 0.60 was achieved. Due to the lower electron density of the benzene unit relative to thiophene, **P14** showed a higher band gap of 1.53 eV and lower HOMO level (−5.35 eV). Because of strong aggregation, the molecular weight of the polymer could not be measured [76]. This low band gap polymer also showed a photo-response up to 800 nm. When combined with $PC_{71}BM$, and its EQE can reach around 40%. Higher PCE of 5.5% with J_{SC} = 10.8 mA/cm^2, V_{OC} = 0.80 V and FF = 0.65 was achieved [76]. Yang et al. also reported a series of new LBG polymers based on DPP unit and the best one is **P15** [77]. By co-polymerizing with a benzo[2,1-b:3,4-b′]dithiophene unit, **P15** shows a small band gap of 1.34 eV and a PCE of 4.45% was achieved with an V_{OC} of 0.72 V, a J_{SC} of 10.0 mA/cm^2, and an FF of 62%. Due to the high performance of DPP based polymers in electronic devices, especially for solar cells, structural modification of the DPP unit was also carried out to explore new materials with even better performance. For example, Frechét et al. and Janssen et al. independently designed and synthesized a series of furan based DPP polymers [78–80]. They showed that by changing the sulfur atom to oxygen atom on the DPP unit, the resulting polymer can achieve similar PV performance and slight increases of V_{OC} were observed. It should be noted that furan derivatives can be synthesized from a variety of natural products; hence, they fall into the category of renewable and sustainable synthetic resources.

One of the furan-DPP based polymers (**P16**) shows a small band gap of 1.41 eV and PCE of 5.0% with J_{SC} = 11.2 mA/cm^2, V_{OC} = 0.74 V and FF = 0.60 [78,79]. Another example is the Thieno[3,2-b]thiophene-based DPP reported by Bronstein et al. They replaced the thiophene unit attached to the DPP core to a thieno[3,2-b]thiophene unit to further increase the mobility of DPP based materials. By co-polymerizing with a thiophene unit, **P17** was obtained with a band gap of 1.37 eV [79]. The maximum hole mobility of 1.95 cm^2 V^{-1} s^{-1} was achieved, which is one of the highest mobilities from a polymer-based OFET reported to date. BHJ solar cells comprising **P17** and $PC_{71}BM$ gave a power conversion efficiency of 5.4% with a V_{OC} of 0.58 V, a J_{SC} of 15.0 mA/cm^2, and a FF of 61%. High EQE of 50% from 350 nm to about 900 nm agrees with the high J_{SC}, caused by the high hole mobility [80]. A new milestone in polymer tandem solar cell research was achieved recently by Yang et al. with a certified PCE of 8.62% [40]. At the core of this breakthrough is the development of a narrow absorption LBG polymer (**P18**, E_g = 1.44 eV), nearly ideal complementary absorption coverage with P3HT. At the heart of this breakthrough is the development of a highly performing LBG polymer (**P18**, E_g = 1.44 eV). A polymer backbone based on the DPP unit and the benzodithiophene (BDT) unit was chosen, building on a previously reported LBG polymer from the same group with a promising band gap of 1.34 eV [77]. By replacing the oxygen atoms attached to the BDT unit with thiophene moieties to form the thienyl benzodithiophene (BDTT) unit, the HOMO and LUMO levels of **P18** are simultaneously shifted deeper (−5.30/−3.63 eV vs. −5.16/−3.51 eV) to increase V_{OC} without losing the driving force for efficient charge separation. Bulkier 2-ethylhexyl side chains on BDTT and 2-butyloctyl side chains on DPP are used to increase the solubility of the resulting polymers and thus obtain much higher molecular weights (40.7 kDa vs. 8.5 kDa). Compared to PBDT-DPP, PBDTT-DPP showcased improved solubility, higher molecular weight, and higher carrier mobility (3.1×10^{-4} cm^2 V^{-1} s^{-1} vs. 6.6×10^{-5} cm^2 V^{-1} s^{-1}, by SCLC method). All these lead to a significantly higher J_{SC} in single-junction devices. Power conversion efficiencies around 6.5% were achieved in single-junction devices with both a regular and an inverted structure (V_{OC} = 0.74 V, J_{SC} = 13.5 mA/cm^2, FF = 65%). When combined with the highly efficient front cell based on P3HT:ICBA and an efficient interconnecting layer of PEDOT:PSS/ZnO in an inverted tandem device configuration, high V_{OC} of 1.56 V, high J_{SC} of 8.26 mA/cm^2 and high FF of 0.67 were obtained simultaneously, and a record 8.62% PCE polymer tandem solar cell (Fig. 4) was achieved. The EQE of the rear cell from 650 nm to 850 nm has a peak value around 50%, which still has much room to improve. A polymer with broader absorption (up to 900 nm) and higher EQE in the NIR region will further enhance the J_{SC} and PCE.

Except BT and DPP, other electron acceptor units were also developed to make new LBG polymers in recent years. Isoindigo has strong electron–withdrawing character due to its two lactam rings. It also has been widely used in the dye industry and can be obtained easily from various natural sources. Isoindigo-based LBG polymers were independently reported by several groups [81–83], with moderate PV performance registered. Very recently, an easily accessible alternating copolymer of terthiophene and isoindigo, **P19**, was designed and synthesized. The polymer presents a promising absorption spectrum (E_g = 1.5 eV) and appropriate HOMO/LUMO positions, leading to a PCE up to 6.3% in the resulting PSCs with V_{OC} of 0.70 V, J_{SC} of 13.1 mA/cm^2, and FF of 69%. Fused BT (NT) and nitrogen atom containing thiadiazolo[3,4-c]pyridine (PT) units were also applied to synthesis of LBG polymers for PV application. Polymer **P20** based on NT unit was reported by Cao et al. [84] and polymers **P21**–**P23** based on PT unit were reported by You et al. [85–88]. All of these polymers showed similar band gap of 1.5 eV and high PV performance of about 6% PCE, due a relatively higher V_{OC} (typically over 0.8 V).

As discussed in this part, LBG polymers with band gap around 1.4 eV (±0.1 eV) are very promising for application in tandem solar cells. The properties of these materials are summarized in Table 2, and the chemical structures are drawn in Fig. 8. For current matching (10 mA/cm^2), it is only required that their EQE reach around 70% from 650

Table 2
The parameters of low bandgap polymers (**P8**–**P26**).

Polymer	E_g^{opt} (eV)	HOMO/LUMO (eV) by CV	V_{OC} (V)	J_{SC} (mA/cm^2)	FF (%)	PCE (%) (single)	PCE (%) (tandem)	References
P8	1.40	−5.30/−3.57	0.62	16.2	55	5.5	6.5	[39,66,67]
P9	1.45	−5.05/−3.27	0.68	12.7	55	5.1	7.0	[42,68,69]
P10	1.37	N.A.	0.57	17.3	61	5.9		[70]
P11	1.43	−4.81/−3.08	0.54	11.9	44	2.8		[71]
P12	1.40	−5.10/−3.40	0.61	11.3	58	4.0	4.9	[56,73,74]
P13	1.30	−5.17/−3.61	0.65	11.8	60	4.7		[75]
P14	1.53	−5.35/−3.53	0.80	10.8	65	5.5		[76]
P15	1.34	−5.21/−3.63	0.72	10.0	62	4.5		[77]
P16	1.41	−5.4/−3.8	0.74	11.2	60	5.0		[78,79]
P17	1.35	−5.06/−3.68	0.58	15.0	61	5.4		[80]
P18	1.44	−5.30/−3.63	0.74	13.5	65	6.5	8.6	[40]
P19	1.50	−5.82/−3.83	0.70	13.1	69	6.3		[81–83]
P20	1.58	−5.19/−3.26	0.80	11.7	61	6.0		[84]
P21	1.53	−5.36/−3.42	0.71	14.1	62	6.2		[85]
P22	1.56	−5.50/−3.44	0.75	13.5	55	5.6		[86]
P23	1.51	−5.47/−3.44	0.85	12.8	58	6.3		[87,88]
P24	1.2	N.A.	0.5	0.9	64	0.23	0.57	[38,89]
P25	1.13	−4.9/−3.63	0.38	14.9	48	2.7		[70]
P26	1.29	−5.04/−3.47	0.55	7.5	51	2.1		[77]

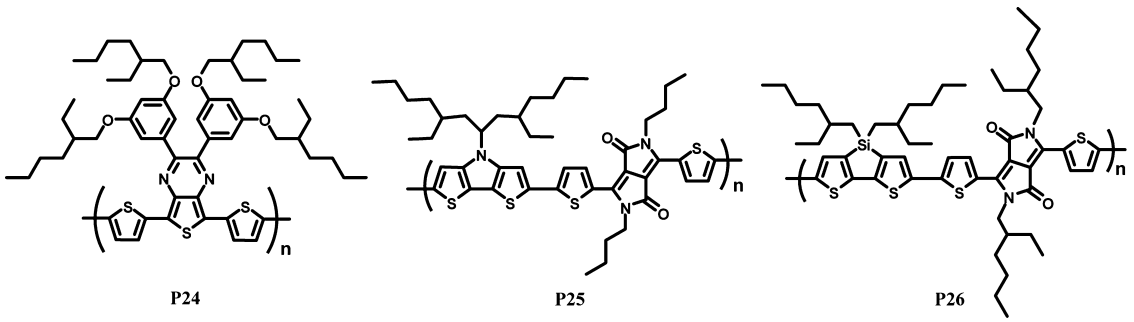

Fig. 9. The chemical structures of low bandgap polymers with a bandgap less than 1.3 eV.

to 800 nm (~1.5 eV) or around 60% from 650 to 850 nm (~1.4 eV) or around 50% from 650 to 900 nm (~1.3 eV). Once such a material is obtained, together with an optimized V_{OC} and FF, the tandem device could reach ~12% PCE (assuming V_{OC} = 1.7 V, J_{SC} = 10 mA/cm^2, FF = 70%). This is a very realistic target. Based on the existing material systems, a modest 10% higher EQE enhancement will do the job. The improvement can come from both materials and optical design. Moreover, according to a theoretical calculation on a double junction tandem cell, once an ideal WBG cell material with a 1.7 eV band gap and an ideal LBG cell material with 1.3 eV are developed, the J_{SC} can reach ~13 mA/cm^2 and peak PCE of 15% could be obtained. The most critical problem that must be overcome to achieve this theoretical limit is still the development of a LBG polymer with a band gap of 1.3 eV with an EQE of ~ 70% or higher.

3.2.2. Polymers with a band gap less than 1.3 eV

Presently, simulated results for tandem polymer solar cells are based on the double-junction tandem structure, and the optimal band gaps for double-junction tandem solar cells are 1.6 and 1. 3 eV, respectively. However, as in inorganic tandem solar cells, moving to a triple-junction architecture is another way to achieve higher performance. In tandem OPV, the synthesis of ultra-low band gap (ULBG) polymers for PV application deserves to be an important direction. At present, one well-known ULBG polymer **P24** (E_g = 1.2 eV) was developed and applied into tandem solar cell in 2006 by Janssen et al. (Fig. 9) [38,89]. In their tandem device, the combination of **P1**/PCBM as the front cell (wide band gap)and **P24**/PCBM as the rear cell (low band gap) with an optimized optical and electronic coupling of the two cells results in 0.57% PCE, which is 1.6 times higher than that of the front cell (0.35%) and 2.5 times higher than that of the rear cell (0.23%).Polymers with similar band gap have also been reported by other groups but the photovoltaic performances were still low. Interestingly, some of them can be used as high performance NIR photo detector active materials. Later on, two ULBG polymers based on the DPP unit (**P25** and **P26**) were developed by Hashimoto et al. [90] and Yang et al. [77] showing enhanced PV performance. Over 2% PCE have been achieved for **P25** and **P26**, but they are still far away from expected value. The reasons for the low PCE could be attributed to three factors: (1) low band gap leads to very low V_{OC} (0.3–0.5 V), wasting most of the energy via a thermalization process; (2) the phase separation between polymer and PCBM is not well controlled to achieve ideal morphology, which leads to poor charge separation and transport; (3) some of them show very low LUMO levels which would be necessary for large V_{OC}, but the LUMO offset between polymer and PCBM may be not enough for charge separation at the interface [19].

3.3. Medium band gap polymers (E_g ~1.6 eV)

Polymers with band gap around 1.6 eV have been champions in single junction polymer solar cells in the last 2–3 years. Great efforts from chemists have lead to simultaneous enhancement of both photocurrent and photovoltage compared to last generation P3HT. Combining materials synthesis with morphology control, the performance of single junction polymer solar cells have been doubled from 4% to over 8%, which still represents the state-of-art. Energy loss due to thermalization was significantly reduced. Here we will review the progress to date and discuss how can they be used in tandem architecture for further performance enhancement.

Novel conjugated polymer (**P27**) based on thienothiophene (TT) and benzodithiophene (BDT) alternating units was first reported by Yu et al. in 2009 (Fig. 10) [91,92]. This polymer exhibits a small band gap of 1.62 eV, because the TT moiety can stabilize the quinoidal structure and lead to a narrow band gap. Preliminary results on this material were promising. PCE as high as 5.6% was achieved with morphology optimization [92]. The pristine material showed a hole mobility of approximately10^{-4} cm^2 V^{-1} s^{-1}. The spectral response of the cell reaches 760 nm (comparing to 650 nm of P3HT) with peak EQE close to 70%, and it is the first polymer system with the EQE comparable or higher than the classical P3HT cell. The short circuit current density was one of the best in the field at 15.6 mA/cm^2. This represents a 50% enhancement over P3HT cells. Because of the position of the HOMO energy level (−4.90 eV) is high, the V_{OC} was 0.56 V. It is comparable to that to P3HT cells but there is still room for further improvements. Indeed, within one year, Yu and Li et al. [18,94,95] and Hou et al. [17,93] reported a series of new polymers based on this backbone (**P28**–**P29**). By changing the ester group to a ketone side chain (**P28**) and adding a fluorine atom on the TT unit (**P29** and **P30**), the HOMO level was moved down to around −5.2 eV and V_{OC}

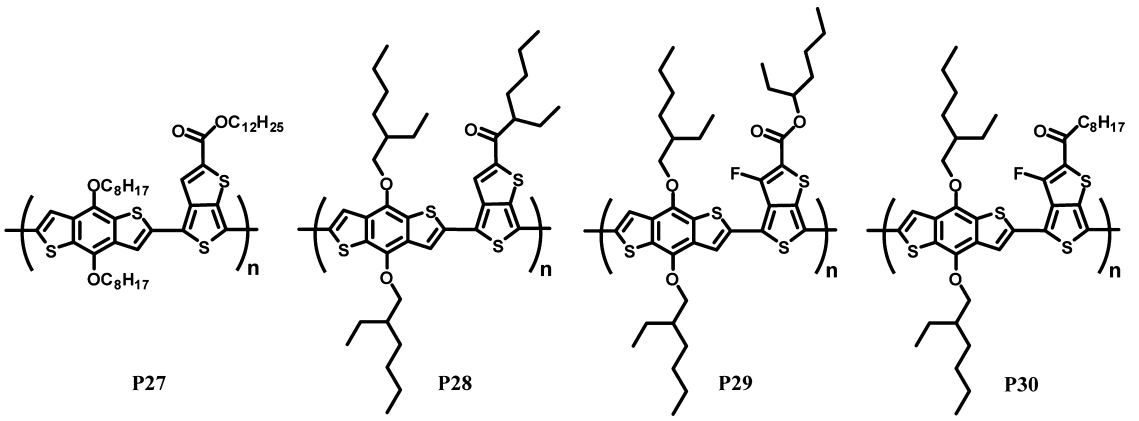

Fig. 10. The chemical structures of PTB series medium bandgap polymers.

Table 3
The performance of medium bandgap polymer solar cells.

Polymer	E_g^{opt} (eV)	HOMO/LUMO (eV) by CV	V_{OC} (V)	J_{SC} (mA/cm^2)	FF (%)	PCE (%)	References
P27	1.58	−4.90/−3.20	0.58	12.5	65.4	4.76	[91,92]
P28	1.61	−5.12/−3.55	0.70	14.7	64	6.58	[93]
P29	1.60	−5.15/−3.31	0.74	14.5	69.0	7.40	[18]
P30	1.61	−5.22/−3.45	0.76	15.2	66.9	7.73	[17]

was increased up to 0.76 V. By optimizing device fabrication using DIO as an additive, PCEs as high as 7.4% (**P29**) and 7.7% (**P30**) were obtained, respectively. The details of **P27**–**P30** are summarized in Table 3. And recently, Cao et al. incorporated a polyelectrolyte as an electron transport layer in the inverted single junction device and 9.2% PCE was achieved for the devices based on **P29**, which is the highest reported value for a single junction polymer solar cell [15]. This clearly indicates the potential for achieving higher performance through a combined molecular engineering and device engineering approach.

Although high efficiencies have been achieved for single junction devices based on **P27**–**P30**, their potential to be applied in tandem devices as LBG cells is limited due to the absorption overlap with the WBG cell material. For example, as shown in Fig. 6, P3HT absorbs up to 650 nm and **P29** (**P30**) absorbs up to 760 nm. Between 650 and 760 nm, the maximum current that can be captured is about 6 mA/cm^2 with EQE = 80%. Even if we can provide a short current of 3 mA/cm^2 from 300 to 650 nm through device engineering current matching, the total current attainable is ~9 mA/cm^2. The highest EQE for **P29** and **P30** is around 75% [17,18,94], therefore the highest current they could provide in tandem device is about 8 mA/cm^2. Assuming V_{OC} = 1.7 V and FF = 0.7, the PCE is estimated to be 9.5%.

A paradigm changing possibility, however, is to use these types of polymer as the front cell candidate. As in the simulation performed by Brabec et al., a high performance tandem solar cell can be achieved by combination of front and rear cells with band gaps of 1.6 and 1.3 eV, respectively, and the power conversion efficiency that could be achieved is about 15%, which is based on the assumption that quantum efficiency and fill factor are both 65% in both sub-cells. BDT-TT based polymers (with a band gap of ~1.6 eV, V_{OC} of 0.74 V, EQE and FF both over than 65%) can be very suitable for the front cells for high efficiency tandem solar cells toward 15% efficiency. The missing component is the high efficiency polymer with a band-gap of ~1.3 eV, which should be identified as a critical research area for OPV. To summarize the status, the state of the art tandem solar cells are based on a wide band gap polymer with a band gap (1.9 eV) and a low band gap polymer with a band gap about 1.4 eV. In the future, high performance tandem solar cells using a medium band gap polymer in the front cell will be achieved after a high quality ultra low band gap polymer is developed.

4. Tandem device engineering and measurement

4.1. Interconnecting layer for polymer tandem solar cells

In the tandem solar cell structure, the interconnecting layer(s) (ICL) connects more than two sub-cells. Ideally, the ICL and sub-cells should form ohmic contact, and the ICL also functions as a charge recombination layer to complete the circuit so that the V_{OC}'s can be added up. In inorganic tandem solar cells, the interconnecting layer is a tunneling diode consisting of heavily doped n and p-type layers. In their organic counterparts, small molecule tandem solar cells are simpler because the interconnecting layer and the top sub-cell are thermally evaporated. For example, Leo et al. evaporated highly p-doped N,N′-diphenyl-N,N′-bis(4′-(N,N-bis(naphth-1-yl)-amino)-biphenyl-4-yl)-benzidine (DiNPB) and n-doped C_{60} directly connecting two cells as a recombination layer [29]. The main limitation of the evaporation approach is its equipment and cost.

However, solution processed polymer tandem cells have different challenges. In addition to optical transparency and electrical functionality, the interconnection

layer coating should not damage the existing sub-cell. As one can imagine, the solvent selection is critical. Once coated, the ICL should also provide protection so that the sequential BHJ active layer coating of the second polymer solar cell will not damage the underlying layers. Therefore, the interconnecting layer should have robustness in addition to device functionality.

The knowledge regarding interfacial layers accumulated in OLED and OPV research provided strong support for tandem OPV interconnecting layer development. The commonly used n-type interfacial layer materials include fluorides (LiF [96,97], CsF [98], etc.), metal oxides (TiO_x [99], ZnO [100], etc.), acetyl acetoneates ($Ca(acac)_2$ [101], etc.), carbonates (Cs_2CO_3 [102,103], etc.), organic small molecules [29], polymers [104,105], self assembled monolayers [106], etc. Cs_2CO_3, ZnO and TiO_x can also modify the electrode work function to form inverted polymer solar cells [107–109]. For polymer electronics, PEDOT:PSS may be the most popular p-type interfacial layer. More recently, various transition metal oxides (TMO) [47,110,111] – NiO, V_2O_5, MoO_3 and WO_3 were introduced in polymer PV as p-type interfacial layers with encouraging OPV results reported using solution processed TMOs [112,113].

In 2006, Kawano et al. demonstrated a polymer tandem solar cell using sputtered ITO combined with PEDOT:PSS as inter-connecting layer [114]. However, there was loss in V_{OC} of the tandem cell compared to the reference single cells because of the high contact resistance at the ITO and bottom cell interface. Then Janssen et al. showcased an efficient ICL consisting of n-type and p-type layers, where the n-type layer is a bi-layer structure (LiF(5 Å)/Al(5 Å)) and the p-type layer is a bi-layer of Au(15 nm)/PEDOT(60 nm) [38]. Based on this ICL, the tandem cell V_{OC} became the sum of the two sub cells. The disadvantage of this structure is also clear. The metal (Au) layer in the ICL is too thick, which leads to loss in transmittance of photons for the rear cell. In addition, both the p and n layers are formed through vacuum deposition, not all solution processed. Solution-processed electron transport layers such as ZnO and TiO_2 have been used as n-type interlayer in single junction polymer solar cells [108,109,111,113,115–117]. These electron transport layers are wide band gap semiconductors and are highly transparent in the visible and NIR wavelength range where the polymer solar cells absorb. On the p-type side, PEDOT:PSS is an excellent hole transport layer for polymer solar cells [118]. Based on these, Gilot et al. demonstrated the first all-solution processed polymer tandem cells [34]. They used zinc oxide (ZnO) nanoparticles (NPs) dissolved in acetone for the deposition of the n-type layer. To avoid the damage to the ZnO layer by acid, neutral pH PEDOT was used as the p-type layer. In the final structure, the solution of ZnO NPs does not damage the bottom polymer layer and the aqueous based neutral PEDOT:PSS layer does not affect the ZnO layer. The thickness of the ZnO layer in the optimized structure was 30 nm and PEDOT thickness was 15 nm. Such an interconnecting layer therefore protects the bottom polymer cell from subsequent solution process. The entire fabrication process was such that none of the solution process steps damaged the layers underneath. Using these solution processed interconnecting layers, double and triple junction tandem cells were shown with minor losses in V_{OC}. Heeger et al. and Yang et al. used stable TiO_2 layer for efficient electron extraction from the bottom cell and the common PEDOT:PSS layer was used as a p-type layer [39,49]. It has been reported that the regular PEDOT:PSS layer is not strong enough to provide protection. The solution to this problem is using a low boiling temperature solvent (e.g. chloroform) for the deposition of the second cell. High performance polymer solar cells are typically based on 1,2-Dichlorobenzene (ODCB) or chlorobenzene (CB) because they can facilitate morphology development for effective charge transport and collection. To overcome the challenge of making high performance tandem solar cells using higher boiling point solvent, Yang et al. introduced surfactant and dimethylformamide (DMF) into PEDOT:PSS to improve the mechanical properties and the conductivity of PEDOT:PSS. The modified PEDOT:PSS layer became very robust and showed the excellent electrical conductivity and transparency [40,52]. High performance low band gap polymer (PBDTT-DPP) processed using DCB as solvent has been successfully used as the second cell, and no damage to the interconnection layer and first cell was observed. As a result, 8.62% efficiency was achieved using in the inverted tandem solar cell structure [40]. Recently, in addition to adding surfactant, Huang et al. combined graphene oxide (GO) and PEDOT:PSS layers to improve the stickiness of the PEDOT:PSS layer for tandem solar cell application [119].

4.2. Tandem solar cells measurement

Accurate characterization of power conversion efficiency (PCE) is essential for the development of solar cell technology. Measurement theory has been developed as early as 1980s. However, as an emerging PV technology, the OPV community has gone through a learning experience first with single junction and more recently with tandem devices. Spectral mismatch correction is at the core of accurate measurement of solar cell efficiency. It is particularly important for OPV as there are no sufficiently stable OPV devices that can serve as reference cells yet. Therefore the difference in spectral response of tested and reference cells, and the difference between the solar simulator spectrum and standard AM spectrum will lead to spectral mismatch. More detailed discussion has been published in 2006 as a joint effort between our group and NREL. Determination of device area is also important. However, it is straight forward if care is taken. Therefore it will not be discussed in this paper. Interested readers are encouraged to refer to some earlier publications [120,121].

Tandem-cell measurement is much more complicated than that of single-junction cells. In principle, each device junction must behave the same under the simulator spectrum as it would have behaved under the reference spectrum (AM1.5G). This requires a spectrum adjustable solar simulator, and significant adjustment of the simulator spectrum. This is typically not available in an individual academic lab. The measurement process is traditionally a tedious iterative process that involves repeatedly calculating spectral mismatch of each junction under a spectrum and changing the filter to adjust spectrum in each run.

To calculate the mismatch of each cell, EQE of tandem solar cells should be measured. For the tandem devices, measuring EQE of these cells using the standard EQE characterization method for single cells is not enough, since the sub-cells work in a collaborative way to utilize different parts of solar spectrum. The optical response of each sub-cell in the tandem structure should be balanced over the entire solar spectrum and not necessarily at a specific wavelength. The inorganic solar cell community has adopted a modified EQE measurement technique that requires additional light biasing to short one of the sub-cells [122]. A simplified version of this approach has been extended to polymer tandem cells by Kim et al. [39]. A monochromatic light bias was used, which selectively excites one sub-cell such that it is saturated while probing EQE of the other sub-cell. The bias light wavelength is chosen such that the sub-cell under test has negligible absorption at that wavelength. However, Janssen et al. [74] pointed out that EQE measurement using this method is only appropriate when the two sub-cells have shunt resistance large enough such that the photocurrent at finite negative bias does not vary significantly from the short circuit point. This is because when the optically biased sub-cell is saturated, a finite photo-voltage (V+) develops across it. Under the short circuit condition of the tandem cell, an equal amount of negative bias (V) is induced across the current limiting sub-cell. Therefore the EQE of the current limiting sub-cell is in reality being measured under reverse bias conditions. This will lead to overestimation of EQE value if the photocurrent is sensitive to the applied bias. In the tandem solar cell mismatch calculation, only the shape of EQE is required. The EQEs are then used to adjust the solar spectrum.

Recently, NREL installed a major solar simulator upgrade for tandem measurement. The so-called one-sun multi-source simulator (OSMSS) uses nine separate wavelength bands of light to build a spectrum such that the ratio of current for the front cell under the reference spectrum and the simulator spectrum is the same as the ratio of current for the rear cell under the reference spectrum and the simulator spectrum. Once such a spectrum is established, the total irradiance is set with a primary calibrated reference cell. In this way, each device junction behaves the same under the simulator spectrum as it would have behaved under the reference spectrum. Therefore once the EQE of tandem cell has been measured, the spectrum adjustment will be controlled by the software and the measurement will be significantly accelerated.

As a majority of academic labs do not have access to a sophisticated spectrum adjustable solar simulator, careful EQE measurement on each cell can provide rough guidance for research purposes. EQE measurement is a commonly used technique to estimate the J_{SC} of single cells accurately. Although accurate measurement of external quantum efficiency is not easy, however, it could be used for estimation of J_{SC} delivered by the tandem cell. Another advantage of measuring the EQE of the sub-cells is that the current limiting cell can be identified and improvements can be made to optimize the tandem cell performance.

5. Conclusion and perspective

Even in its infancy, polymer tandem solar cell research has been achieved great progress in past five years, with the efficiency now reaching 10% [31]. This sets a milestone for organic solar cell technology as a whole. Significant progress can be expected in the near future in this promising field. The tandem concept opens a new dimension in polymeric semiconducting materials design. Further improvements in interconnecting layers will be critical to support the technology to move to real world application. Many effective techniques developed in single junction polymer solar cells can be applied in tandem structures too. Amount these approaches; those effective in improving external quantum efficiency over a wide spectral band are particularly important. Today, the Mitsubishi Chemicals in Japan has demonstrated ~80% EQE across a broad spectrum [123]. The EQE in state-of-art polymer tandem solar cells is in the 50% range. The promising EQE enhancement candidates may include light trapping through optical effects such as optical spacer and introducing light trapping nanostructures, and plasmonic active nanoparticles [124], 15% efficiency in polymer tandem solar cells could be attained with high EQE only.

Tandem OPV is a very promising research area. Small molecule tandem solar cells have also undergone fast progress. In 2005, Forrest et al. achieved 5.7% efficiency in small molecule tandem solar cells [125]. Now the Heliatek GmbH in Germany have announced 9.8% efficiency in a tandem small molecule solar cell [30], which indicates that the high potential of small molecule tandem solar cells. Recently, ~7% efficiency from solution processed small molecules has been achieved by Heeger and Bazan et al. [126]. There is also wide room for the development of solution processed tandem small molecule solar cells.

Over the last decade, OPV technology has progressed significantly in both polymer and small molecule areas, both solution processed and evaporated. We have enough reasons to believe that technological breakthroughs will continuous to come, and the polymer tandem solar cells are a very promising new frontier for OPV technology to realize their low cost and high efficiency promise.

6. Supplementary

There has been tremendous progress in this fast growing field since the initial submission of this manuscript in 2011. One of the most notable developments is the emergence of low band gap polymers specially designed for tandem solar cells. One typical example is poly[2,7-(5,5-bis-(3,7-dimethyloctyl)-5H-dithieno[3,2-b:2′,3′-d]pyran)-alt-4,7-(5,6-difluoro-2,1,3-benzothia diazole)] (PDTP-DFBT, **P31**), which has a band gap of 1.38 eV. Its chemical structure is shown in Fig. 11(a). The EQE of single junction PDTP-DFBT:fullerene photovoltaic cells reached over 60% in the infrared region [31]. Moreover, when blended with $PC_{71}BM$ and $PC_{61}BM$, The PCEs reached an incredible 7.9% and 7.1%, respectively. The detailed parameters of the photovoltaic cells are summarized in Table 4. As shown in Fig. 11(b), the tandem architecture consists of a PDTP-DFBT rear sub-cell and P3HT front

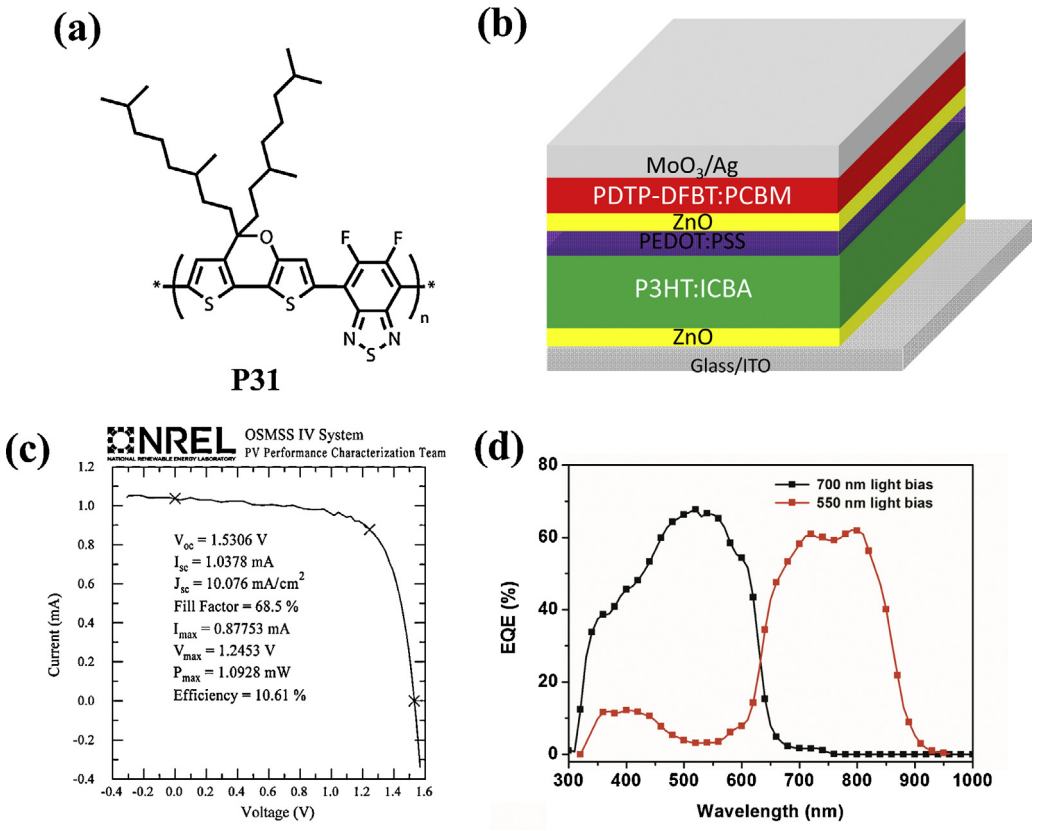

Fig. 11. (a) Chemical structure of **P31** (PDTP-DFBT), (b) the tandem devices structure of a 10.6% polymer tandem solar cells, (c) the *J–V* curve of 10.6% inverted tandem cell as certified by National Renewable Energy Laboratory (NREL), and (d) External quantum efficiency of the 10.6% polymer tandem solar cells [31].

sub-cell. Since the absorption bands of PDTP-DFBT and P3HT are well separated, the rear sub-cell is responsible for the near-infrared light in the 650–900 nm spectrum; P3HT covers the photons from the near-ultraviolet to 650 nm spectrum. Therefore, a high short-circuit current can be attained in the tandem cell, and a certificated power conversion efficiency of 10.6% has thus been achieved [31]. The certified *I–V* from NREL is shown in Fig. 11(c) and the quantum efficiency of the corresponding device is shown in Fig. 11(d). This breakthrough progress sets a new record efficiency in the OPV field [31].

In accordance with such innovative progress, this high performance PDTP-DFBT and $PC_{71}BM$ polymer-blend is also being used to form a new and unique homogeneous tandem structure, which contains two identical sub-cells [127]. The homogeneous tandem solar cell provides a solution to resolve the low carrier mobility of organic compounds. It enhances the optical absorption via stacking two or more layers of active layer, while maintaining the charge transport and collection within it. However, the homogeneous tandem cell cannot reduce the thermal loss realized with the traditional tandem solar cells stacking active layer with complementary absorption [31]. The PCE of the identical sub-cell-based tandem cells is still limited by the Shockley–Queisser theory [24]. Yet considering the low carrier mobility in polymer:fullerene blend film, the HOMO tandem architecture has a higher chance to enhance both internal quantum efficiency (IQE) and EQE of the PSCs.

Other modification polymers introduced by Yang et al. [128] and Janssen et al. [129] include PBDTT-SeDPP (**P32**) and poly[[2,5-bis(2-hexyldecyl-2,3,5,6-tetrahydro-3,6-dioxopyrrolo[3,4-c]pyrrole-1,4-diyl]-alt-[3′,3″-dimethyl-2,2′:5′,2″-terthiophene]-5,5″-diyl] (PMDPP3T, **P33**), which are based on (PBDTT-DPP, **P18**) and (PDPP3T, **P13**), respectively. The chemical structures of **P32** and **P33** are shown in Fig. 12. The polymer PBDTT-SeDPP (E_g = 1.38 eV) shows

Table 4
New low bandgap polymer designed for tandem solar cells.

Polymer	E_g^{opt} (eV)	HOMO/LUMO (eV) by CV	V_{OC} (V)	J_{SC} (mA/cm^2)	FF (%)	PCE (%) (single)	PCE (%) (tandem)	References
P31	1.38	−5.26/−3.61	0.68	17.8	65	7.9	10.6	[31]
P32	1.38	−5.25/−3.70	0.69	16.8	62	7.2	9.5	[128]
P33	1.30	−5.24/−3.61	0.60	17.8	66	7.0	8.9	[129]

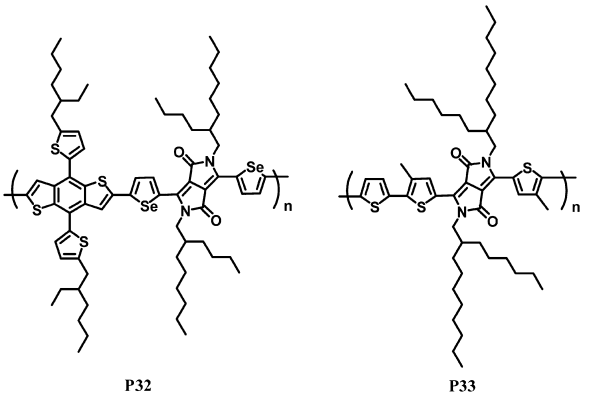

Fig. 12. The chemical structure of two high efficiency low bandgap polymer **P32** (PBDTT-SeDPP) and **P33** (PMDPP3T).

excellent photovoltaic performance in single junction devices, with PCEs over 7% and photo-response up to 900 nm. Combining this low-band gap sub-cell polymer band gap with P3HT to yield a wide band gap sub-cell in tandem structure, the device yields a 9.5% power conversion efficiency. In comparison with PDPP3T, the single junction power conversion efficiency improved from band gap 4.7% to 7% for the low band gap PMDPP3T; use of this polymer in the rear cell for tandem solar cells, resulted in an efficiency of 8.9%. The power conversion efficiency was further improved to 9.64% when a triple junction structure was employed to harvest as much light as possible. The detailed parameters of the photovoltaic cells based on **P32** and **P33** are also summarized in Table 4. In spite of the fact that EQE characterization of triple junction cells is technically challenging, especially when two of the three junctions are based on the same material, optical simulation provides a reliable solution to estimate the absorption and photocurrent balance within the multi-junction structure.

In the years of 2012 and 2013, immense progress was achieved in techniques for small molecular multi-junctions via vacuum deposition. In April 2012, Heliatek GmbH, a company located in Dresden, Germany [30], announced power conversion efficiency of 10.7% from dual-junction tandem cells based on small molecules. More recently, they achieved a 12% power conversion efficiency based on triple junction OPV cells [30]. Hence, this application of organic doping proves to be a success with OPV cells [130].

In light of these development trends, triple junctions provide a powerful approach for achieving >15% efficiency by reducing thermal loss, which could be utilized to improve the overall effective absorption in the near future.

Acknowledgements

This work was financially supported by the Air Force Office of Scientific Research (AFOSR, Grant No. FA9550-09-1-0610, Program manager: Dr. Charles Lee), Office of Naval Research (ONR, Grant No. N00014-04-1-0434, Program manager: Dr. Paul Armistead), and National Science Foundation (NSF, Grant No. CHE0822573, Program manager: Colby Foss). The authors would like to thank *Royal Society of Chemistry* (RSC) allow us to reproduce the materials therein (Ref. [21]). The authors also would like to thank Eric Richard for proof reading the manuscript.

References

[1] Chapin DM, Fuller CS, Pearson GL. A new silicon p–n junction photocell for converting solar radiation into electrical power. J Appl Phys 1954;25:676–7.
[2] Yu G, Gao J, Hummelen JC, Wudl F, Heeger AJ. Polymer photovoltaic cells-enhanced efficiencies via a network of internal donor–acceptor heterojunctions. Science 1995;270:1789–91.
[3] Shaheen SE, Brabec CJ, Sariciftci NS, Padinger F, Fromhez T, Hummelen JC. 2.5% efficient organic plastic solar cells. Appl Phys Lett 2001;78:841–3.
[4] Peumans P, Yakimov A, Forrest SR. Small molecular weight organic thin-film photodetectors and solar cells. J Appl Phys 2003;93:3693–723.
[5] Brabec CJ, Sariciftci NS, Hummelen JC. Plastic solar cells. Adv Funt Mater 2001;11:15–26.
[6] Guenes S, Neugebauer H, Sariciftci NS. Conjugated polymer-based organic solar cells. Chem Rev 2007;107:1324–38.
[7] Thompson BC, Frechet JMJ. Organic photovoltaics-polymer-fullerene composite solar cells. Angew Chem Int Ed 2008;47:58–77.
[8] Bundgaard E, Krebs FC. Low band gap polymers for organic photovoltaics. Sol Energy Mat Sol C 2007;91:954–85.
[9] Dennler G, Scharber MC, Brabec CJ. Polymer-fullerene bulk-heterojunction solar cells. Adv Mater 2009;21:1323–38.
[10] Chen LM, Hong ZR, Li G, Yang Y. Recent progress in polymer solar cells: manipulation of polymer:fullerene morphology and the formation of efficient inverted polymer solar cells. Adv Mater 2009;21:1434–49.
[11] Li G, Shrotriya V, Yao Y, Huang JS, Yang Y. Manipulating regioregular poly(3-hexylthiophene):[6,6]-phenyl-C61-butyric acid methyl ester blends—route towards high efficiency polymer solar cells. J Mater Chem 2007;17:3126–40.
[12] Coakley KM, McGehee MD. Conjugated polymer photovoltaic cells. Chem Mater 2004;16:4533–42.
[13] Li G, Shrotriya V, Huang JS, Yao Y, Moriarty T, Emery K, Yang Y. High-efficiency solution processable polymer photovoltaic cells by self-organization of polymer blends. Nat Mater 2005;4:864–8.
[14] Ma WL, Yang CY, Gong X, Lee K, Heeger AJ. Thermally stable, efficient polymer solar cells with nanoscale control of the interpenetrating network morphology. Adv Funt Mater 2005;15:1617–22.
[15] He ZC, Zhong CM, Su SJ, Xu M, Wu HB, Cao Y. Enhanced power-conversion efficiency in polymer solar cells using an inverted device structure. Nat Photonics 2012;6:591–5.
[16] Small CE, Chen S, Subbiah J, Amb C, Tsang SW, Lai TH, Reynolds JR, So F. High-efficiency inverted dithienogermole–thienopyrrolodione-based polymer solar cells. Nat Photonics 2012;6:115–20.
[17] Chen HY, Hou JH, Zhang SQ, Liang YY, Yang GW, Yang Y, Yu LP, Wu Y, Li G. Polymer solar cells with enhanced open-circuit voltage and efficiency. Nat Photonics 2009;3:649–53.
[18] Liang YY, Xu Z, Xia JB, Tsai ST, Wu Y, Li G, Ray C, Yu LP. For the bright future-bulk heterojunction polymer solar cells with power conversion efficiency of 7.4%. Adv Mater 2010;22:E135–8.
[19] Scharber MC, Wuhlbacher D, Koppe M, Denk P, Waldauf C, Heeger AJ, Brabec CJ. Design rules for donors in bulk-heterojunction solar cells - Towards 10% energy-conversion efficiency. Adv Mater 2006;18:789–94.
[20] Koster LJA, Mihailetchi VD, Blom PWM. Ultimate efficiency of polymer/fullerene bulk heterojunction solar cells. Appl Phys Lett 2006;88, 093511/1–3.
[21] Sista S, Hong ZR, Chen LM, Yang Y. Tandem polymer photovoltaic cells—current status, challenges and future outlook. Energy Environ Sci 2011;4:1606–20.
[22] Sista S, Hong ZR, Park MH, Xu Z, Yang Y. High-efficiency polymer tandem solar cells with three-terminal structure. Adv Mater 2010;22:E77–80.
[23] Ameri T, Dennler G, Lungenschmied C, Brabec CJ. Organic tandem solar cells: a review. Energy Environ Sci 2009;2:347–63.
[24] Shockley W, Queisser HJ. Detailed balance limit of efficiency of p-n junction solar cells. J Appl Phys 1961;32:510–9.
[25] Green MA, Emery K, Hishikiwa Y, Warta W, Dunlop ED. Solar cell efficiency tables (version 39). Prog Photovoltaics 2011;20:12–20.
[26] Dennler G, Scharber MC, Ameri T, Denk P, Forberich K, Waldauf C, Brabec CJ. Design rules for donors in bulk-heterojunction tandem

solar cells-towards 15% energy-conversion efficiency. Adv Mater 2008;20:579–83.
[27] Wienk MM, Kroon JM, Verhees WJH, Knol J, Hummelen JC, van Hal PA, Janssen RAJ. Efficient methano[70]fullerene/MDMO-PPV bulk heterojunction photovoltaic cells. Angew Chem Int Ed 2003;42:3371–5.
[28] Yakimov A, Forrest SR. High photovoltage multiple-heterojunction organic solar cells incorporating interfacial metallic nanoclusters. Appl Phys Lett 2002;80:1667–9.
[29] Riede M, Uhrich C, Widmer J, Timmreck R, Wynands D, Schwartz G, Gnehr WM, Hildebrandt D, Weiss A, Hwang J, Sundarraj S, Erk P, Pfeiffer M, Leo K. Efficient organic tandem solar cells based on small molecules. Adv Funt Mater 2011;21:3019–28.
[30] Anonymous. Hellatek website; 2012 http://www.heliatek.com/ (accessed May 2013).
[31] You JB, Dou LT, Yoshimura K, Kato T, Ohya K, Moriarty T, Emery K, Chen CC, Gao J, Li G, Yang Y. A polymer tandem solar cell with 10.6% power conversion efficiency. Nat Commun 2013;4, 1446/1–10.
[32] Shrotriya V, Wu EHE, Li G, Yao Y, Yang Y. Efficient light harvesting in multiple-device stacked structure for polymer solar cells. Appl Phys Lett 2006;88, 064104/1–3.
[33] Zhao DW, Sun XW, Jiang CY, Kyaw AKK, Lo GQ, Kwong DL. An efficient triple-tandem polymer solar cell. IEEE Electron Dev Lett 2009;30:490–2.
[34] Gilot J, Wienk MM, Janssen RAJ. Double and triple junction polymer solar cells processed from solution. Appl Phys Lett 2007;90, 143512/1–3.
[35] Dennler G, Prall HJ, Koeppe R, Egginger M, Autengruber R, Sariciftci NS. Enhanced spectral coverage in tandem organic solar cells. Appl Phys Lett 2006;89, 073502/1–3.
[36] Zhao DW, Sun XW, Jiang CY, Kyaw AKK, Lo GQ, Kwong DL. Efficient tandem organic solar cells with an Al/MoO3 intermediate layer. Appl Phys Lett 2008;93, 083305/1–3.
[37] Colsmann A, Junge J, Kayser C, Lemmer U. Organic tandem solar cells comprising polymer and small-molecule subcells. Appl Phys Lett 2006;89, 203506/1–3.
[38] Hadipour A, de Boer B, Wildeman J, Kooistra F, Hummelen JC, Turbiez MGR, Wienk MM, Janssen RAJ, Blom PWM. Solution-processed organic tandem solar cells. Adv Funt Mater 2006;16: 1897–903.
[39] Kim JY, Lee K, Coates NE, Moses D, Nguyen TQ, Dante M, Heeger AJ. Efficient tandem polymer solar cells fabricated by all-solution processing. Science 2007;317:222–5.
[40] Dou LT, You JB, Yang J, Chen CC, He YJ, Murase S, Moriarty T, Emery K, Li G, Yang Y. Tandem polymer solar cells featuring a spectrally-matched low bandgap polymer. Nat Photonics 2012;6:180–5.
[41] Peet J, Kim JY, Coates NE, Ma WL, Moses D, Heeger AJ, Bazan GC. Efficiency enhancement in low-bandgap polymer solar cells by processing with alkane dithiols. Nat Mater 2007;6:497–500.
[42] Hou JH, Chen HY, Zhang SQ, Li G, Yang Y. Synthesis, Characterization, and Photovoltaic Properties of a Low Band Gap Polymer Based on Silole-Containing Polythiophenes and 2,1,3-Benzothiadiazole. J Am Chem Soc 2008;130:16144–5.
[43] Ye L, Zhang SQ, Ma W, Fan BH, Guo X, Huang Y, Ade H, Hou JH. From binary to ternary solvent: morphology fine-tuning of d/a blends in pdpp3t-based polymer solar cells. Adv Mater 2012;24: 6335–41.
[44] Wudl F, Srdanov G. Conducting polymer formed of poly(2-methoxy-5-(2'-ethylhexyloxy)-p-phenylene vinylene). US Pat 5,189,136, 1993.
[45] McCullough RD, Williams SP. Toward tuning electrical and optical properties in conjugated polymers using side-chains: the synthesis and physical properties of a series of the first head-to-tail heteroatom functionalized polythiophenes. J Am Chem Soc 1993;115:11608–9.
[46] Chen TA, Rieke RD. The first regioregular head-to-tail poly(3-hexylthiophene-2,5-diyl) and a regiorandom isopolymer:nickel versus palladium catalysis of 2(5)-bromo-5(2)-(bromozincio)-3-hexylthiophene polymerization. J Am Chem Soc 1992;114:10087–8.
[47] Sirringhaus H, Brown PJ, Friend RH, Nielsen MM, Bechgaard K, Langeveld-Voss BMW, Spiering AJH, Janssen RAJ, Meijer EW, Herwig P, de Leeuw DM. Two-dimensional charge transport in self-organized, high-mobility conjugated polymers. Nature 1999;401:685–8.
[48] Irwin MD, Buchholz B, Hains AW, Chang RPH, Marks TJ. p-Type semiconducting nickel oxide as an efficiency-enhancing anode interfacial layer in polymer bulk-heterojunction solar cells. PNAS 2008;105:2783–7.
[49] Sista S, Park MH, Hong ZR, Wu Y, Hou JH, Kwan WL, Li G, Yang Y. Highly efficient tandem polymer photovoltaic cells. Adv Mater 2010;22:380–3.
[50] He YJ, Chen HY, Hou JH, Li YF. Indene-C(60) bisadduct: a new acceptor for high-performance polymer solar cells. J Am Chem Soc 2010;132:1377–82.
[51] Zhao GJ, He YJ, Li YF. 6.5% Efficiency of polymer solar cells based on poly(3-hexylthiophene) and indene-c(60) bisadduct by device optimization. Adv Mater 2010;22:4355–8.
[52] Yang J, Zhu R, Hong ZR, He YJ, Kumar A, Li YF, Yang Y. A robust interconnecting layer for achieving high performance tandem polymer solar cells. Adv Mater 2011;23:3465–70.
[53] Mccullough RD, Tristramnagle S, Williams SP, Lowe RD, Jayaraman M. Self-orienting head-to-tail poly(3-alkylthiophenes) - new insights on structure-property relationships in conducting polymers. J Am Chem Soc 1993;115:4910–1.
[54] Yu WL, Meng H, Pei J, Huang W. Tuning redox behavior and emissive wavelength of conjugated polymers by p-n diblock structures. J Am Chem Soc 1998;120:11808–9.
[55] Zhou QM, Hou Q, Zheng LP, Deng XY, Yu G, Cao Y. Fluorene-based low band-gap copolymers for high performance photovoltaic devices. Appl Phys Lett 2004;84:1653–5.
[56] Gilot J, Wienk MM, Janssen RAJ. Optimizing polymer tandem solar cells. Adv Mater 2010;22:E67–71.
[57] Park SH, Roy A, Beaupre S, Cho S, Coates N, Moon JS, Moses D, Leclerc M, Lee K, Heeger AJ. Bulk heterojunction solar cells with internal quantum efficiency approaching 100%. Nat Photonics 2009;3:297–302.
[58] Huo LJ, Hou JH, Zhang SQ, Chen HY, Yang Y. A poly benzo[1,2-b:4,5-b′]dithiophene derivative with deep homo level and its application in high-performance polymer solar cells. Angew Chem Int Ed 2010;49:1500–3.
[59] Price SC, Stuart AC, Yang LQ, Zhou HX, You W. Fluorine substituted conjugated polymer of medium band gap yields 7% efficiency in polymer-fullerene solar cells. J Am Chem Soc 2011;133: 4625–31.
[60] Piliego C, Holcombe TW, Douglas JD, Woo CH, Beaujuge PM, Frechet JMJ. Synthetic control of structural order in n-alkylthieno[3,4-c]pyrrole-4,6-dione-based polymers for efficient solar cells. J Am Chem Soc 2010;132:7595–7.
[61] Zou YP, Najari A, Berrouard P, Beaupre S, Aich BR, Tao Y, Leclerc M. A thieno[3,4-c]pyrrole-4,6-dione-based copolymer for efficient solar cells. J Am Chem Soc 2010;132:5330–1.
[62] Chu TY, Lu JP, Beaupre S, Zhang YG, Pouliot JR, Wakim S, Zhou JY, Leclerc M, Li Z, Ding JF, Tao Y. Bulk heterojunction solar cells using thieno[3,4-c]pyrrole-4,6-dione and dithieno[3,2-b:2 ‘,3 ‘-d]silole copolymer with a power conversion efficiency of 7.3%. J Am Chem Soc 2011;133:4250–3.
[63] Zhang Y, Hau SK, Yip HL, Sun Y, Acton O, Jen AKY. Benzobis(silolothiophene)-based low bandgap polymers for efficient polymer solar cells. Chem Mater 2011;23:765–7.
[64] Amb CM, Chen S, Graham KR, Subbiah J, Small CE, So F, Reynolds JR. Dithienogermole as a fused electron donor in bulk heterojunction solar cells. J Am Chem Soc 2011;133:10062–5.
[65] Cheng YJ, Yang SH, Hsu CS. Synthesis of conjugated polymers for organic solar cell applications. Chem Rev 2009;109:5868–923.
[66] Muhlbacher D, Scharber M, Morana M, Zhu ZG, Waller D, Gaudiana R, Brabec CJ. High photovoltaic performance of a low-bandgap polymer. Adv Mater 2006;18:2884–9.
[67] Lee JK, Ma WL, Brabec CJ, Yuen J, Moon JS, Kim JY, Lee K, Bazan GC, Heeger AJ. Processing additives for improved efficiency from bulk heterojunction solar cells. J Am Chem Soc 2008;130:3619–23.
[68] Chen HY, Hou JH, Hayden AE, Yang H, Houk KN, Yang Y. Silicon atom substitution enhances interchain packing in a thiophene-based polymer system. Adv Mater 2010;22:371–5.
[69] Morana M, Azimi H, Dennler G, Egelhaaf HJ, Scharber M, Forberich K, Hauch J, Gaudiana R, Waller D, Zhu ZH, Hingerl K, van Bavel SS, Loos J, Brabec CJ. Nanomorphology and charge generation in bulk heterojunctions based on low-bandgap dithiophene polymers with different bridging atoms. Adv Funt Mater 2010;20: 1180–8.
[70] Coffin RC, Peet J, Rogers J, Bazan GC. Streamlined microwave-assisted preparation of narrow-bandgap conjugated polymers for high-performance bulk heterojunction solar cells. Nat Chem 2009;1:657–61.
[71] Yue W, Zhao Y, Shao SY, Tian HK, Xie ZY, Geng YH, Wang FS. Novel NIR-absorbing conjugated polymers for efficient polymer solar cells:effect of alkyl chain length on device performance. J Mater Chem 2009;19:2199–206.

[72] Burgi L, Turbiez M, Pfeiffer R, Bienewald F, Kirner HJ, Winnewisser C. High-mobility ambipolar near-infrared light-emitting polymer field-effect transistors. Adv Mater 2008;20:2217–24.
[73] Wienk MM, Turbiez M, Gilot J, Janssen RAJ. Narrow-bandgap diketo-pyrrolo-pyrrole polymer solar cells: the effect of processing on the performance. Adv Mater 2008;20:2556–60.
[74] Gilot J, Wienk MM, Janssen RAJ. Measuring the external quantum efficiency of two-terminal polymer tandem solar cells. Adv Funt Mater 2010;20:3904–11.
[75] Bijleveld JC, Zoombelt AP, Mathijssen SGJ, Wienk MM, Turbiez M, de Leeuw DM, Janssen RAJ. Poly (diketopyrrolopyrrole-terthiophene) for ambipolar logic and photovoltaics. J Am Chem Soc 2009;131:16616–7.
[76] Bijleveld JC, Gevaerts VS, DiNuzzo D, Turbiez M, Mathijssen SGJ, de Leeuw DM, Wienk MM, Janssen RAJ. Efficient solar cells based on an easily accessible diketopyrrolopyrrole polymer. Adv Mater 2010;22:E242–6.
[77] Huo LJ, Hou JH, Chen HY, Zhang SQ, Jiang Y, Chen TL, Yang Y. Bandgap and molecular level control of the low-bandgap polymers based on 3,6-dithiophen-2-yl-2,5-dihydropyrrolo[3,4-c]pyrrole-1,4-dione toward highly efficient polymer solar cells. Macromolecules 2009;42:6564–71.
[78] Woo CH, Beaujuge PM, Holcombe TW, Lee OP, Frechét JMJ. Incorporation of furan into low band-gap polymers for efficient solar cells. J Am Chem Soc 2010;132:15547–9.
[79] Bijleveld JC, Karsten BP, Mathijssen SGJ, Wienk MM, de Leeuw DM, Janssen RAJ. Small band gap copolymers based on furan and diketopyrrolopyrrole for field-effect transistors and photovoltaic cells. J Mater Chem 2011;2:1600–6.
[80] Bronstein H, Chen ZY, Ashraf RS, Zhang WM, Du JP, Durrant JR, Tuladhar PS, Song K, Watkins SE, Geerts Y, Wienk MM, Janssen RAJ, Anthopoulos T, Sirringhaus H, Heeney M, McCulloch I. Thieno[3,2-b]thiophene – Diketopyrrolopyrrole-Containing polymers for high-performance organic field-effect transistors and organic photovoltaic devices. J Am Chem Soc 2011;133:3272–5.
[81] Zhang GB, Fu YY, Xie ZY, Zhang Q. Synthesis and photovoltaic properties of new low bandgap isoindigo-based conjugated polymers. Macromolecules 2011;44:1414–20.
[82] Liu B, Zou YP, Peng B, Zhao B, Huang K, He YH, Pan CY. Low bandgap isoindigo-based copolymers:design, synthesis and photovoltaic applications. Polym Chem 2011;2:1156–62.
[83] Wang EG, Ma ZF, Zhang Z, Henriksson P, Inganas O, Zhang FL, Andersson MR. An isoindigo-based low band gap polymer for efficient polymer solar cells with high photo-voltage. Chem Commun 2011;47:4908–10.
[84] Wang M, Hu XW, Liu P, Li W, Gong X, Huang F, Cao Y. Donor–acceptor conjugated polymer based on ÿaphtha[1,2-c:5,6-c]bis[1,2,5]thiadiazole for high-performance polymer solar cells. J Am Chem Soc 2011;133:9638–41.
[85] Zhou HX, Yang LQ, Price SC, Knight KJ, You W. Enhanced photovoltaic performance of low-bandgap polymers with deep lumo levels. Angew Chem Int Ed 2010;49:7992–5.
[86] Price SC, Stuart AC, You W. Low band gap polymers based on benzo[1,2-b:4,5-b′]dithiophene:rational design of polymers leads to high photovoltaic performance. Macromolecules 2010;43:4609–12.
[87] Zhou HX, Yang LQ, Xiao SQ, Liu SB, You W. Donor–acceptor polymers incorporating alkylated dithienyl benzothiadiazole for bulk heterojunction solar cells: pronounced effect of positioning alkyl chains. Macromolecules 2010;43:811–20.
[88] Blouin N, Michaud A, Gendron D, Wakim S, Blair E, Neagu-Plesu R, Belletete M, Durocher G, Tao Y, Leclerc M. Toward a rational design of poly(2,7-carbazole) derivatives for solar cells. J Am Chem Soc 2008;130:732–42.
[89] Wienk MM, Turbiez MGR, Struijk MP, Fonrodona M, Janssen RAJ. Low-band gap poly(di-2-thienylthienopyrazin): fullerene solar cells. Appl Phys Lett 2006;88, 153511/1–3.
[90] Zhou EJ, Wei QS, Yamakawa S, Zhang Y, Tajima K, Yang CH, Hashimoto K. Diketopyrrolopyrrole-based semiconducting polymer for photovoltaic device with photocurrent response wavelengths up to 1.1 μm. Macromolecules 2010;43:821–6.
[91] Liang YY, Wu Y, Feng DQ, Tsai ST, Son HJ, Li G, Yu LP. Development of new semiconducting polymers for high performance solar cells. J Am Chem Soc 2009;131:56–7.
[92] Liang YY, Feng DQ, Wu Y, Tsai ST, Li G, Ray C, Yu LP. Highly efficient solar cell polymers developed via fine-tuning of structural and electronic properties. J Am Chem Soc 2009;131:7792–9.
[93] Hou JH, Chen HY, Zhang SQ, Chen RI, Yang Y, Wu Y, Li G. Synthesis of a low band gap polymer and its application in highly efficient polymer solar cells. J Am Chem Soc 2009;131:15586–7.
[94] Liang YY, Yu LP. A new class of semiconducting polymers for bulk heterojunction solar cells with exceptionally high performance. Acc Chem Res 2010;43:1227–36.
[95] Son HJ, He F, Carsten B, Yu LP. Are we there yet? Design of better conjugated polymers for polymer solar cells. J Mater Chem 2011;21:18934–45.
[96] Hung LS, Tang CW, Mason MG. Enhanced electron injection in organic electroluminescence devices using an Al/LiF electrode. Appl Phys Lett 1997;70:152–4.
[97] Brabec CJ, Shaheen SE, Winder C, Sariciftci NS, Denk P. Effect of LiF/metal electrodes on the performance of plastic solar cells. Appl Phys Lett 2002;80:1288–90.
[98] Jabbour GE, Kippelen B, Armstrong NR, Peyghambarian N. Aluminum based cathode structure for enhanced electron injection in electroluminescent organic devices. Appl Phys Lett 1998;73:1185–7.
[99] Kim JY, Kim SH, Lee HH, Lee K, Ma W, Gong X, Heeger AJ. New architecture for high-efficiency polymer photovoltaic cells using solution-based titanium oxide as an optical spacer. Adv Mater 2006;18:572–6.
[100] Gilot J, Barbu I, Wienk MM, Janssen RAJ. The use of ZnO as optical spacer in polymer solar cells:theoretical and experimental study. Appl Phys Lett 2007;91, 113520/1–3.
[101] Xu Q, Ouyang J, Yang Y, Ito T, Kido J. Ultrahigh efficiency green polymer light-emitting diodes by nanoscale interface modification. Appl Phys Lett 2003;83:4695–7.
[102] Huang J, Li G, Yang Y. A semi-transparent plastic solar cell fabricated by a lamination process. Adv Mater 2008;20:415–9.
[103] Park MH, Li JH, Kumar A, Li G, Yang Y. Doping of the metal oxide nanostructure and its influence in organic electronics. Adv Funt Mater 2009;19:1241–6.
[104] Yang Y, Pei Q. Electron injection polymer for polymer light-emitting-diodes. J Appl Phys 1995;77:4807–9.
[105] Huang F, Hou LT, Wu HB, Wang XH, Shen HL, Cao W, Yang W, Cao Y. High-efficiency, environment-friendly electroluminescent polymers with stable high work function metal as a cathode: green- and yellow-emitting conjugated polyfluorene polyelectrolytes and their neutral precursors. J Am Chem Soc 2004;126:9845–53.
[106] Yip HL, Hau SK, Baek NS, Ma H, Jen AKY. Polymer solar cells that use self-assembled-monolayer-modified ZnO/metals as cathodes. Adv Mater 2008;20:2376–82.
[107] Li G, Chu CW, Shrotriya V, Huang J, Yang Y. Efficient inverted polymer solar cells. Appl Phys Lett 2006;88, 253503/1–3.
[108] White S, Olson DC, Shaheen SE, Kopidakis N, Ginley DS. Inverted bulk-heterojunction organic photovoltaic device using a solution-derived ZnO underlayer. Appl Phys Lett 2006;89, 143517/1–3.
[109] Waldauf C, Morana M, Denk P, Schilinsky P, Coakley K, Choulis SA, Brabec CJ. Highly efficient inverted organic photovoltaics using solution based titanium oxide as electron selective contact. Appl Phys Lett 2006;89, 233517/1–3.
[110] Shrotriya V, Li G, Yao Y, Chu CW, Yang Y. Transition metal oxides as the buffer layer for polymer photovoltaic cells. Appl Phys Lett 2006;88, 073508/1–3.
[111] Sun YM, Takacs CJ, Cowan SR, Seo JH, Gong X, Roy A, Heeger AJ. Efficient, air-stable bulk heterojunction polymer solar cells using MoOx as the anode interfacial layer. Adv Mater 2011;23:2226–30.
[112] Steirer KX, Ndione PF, Widjonarko NE, Lloyd MT, Meyer J, Ratcliff EL, Kahn A, Armstrong NR, Curtis CJ, Ginley DS, Berry JJ, Olson DC. Enhanced efficiency in plastic solar cells via energy matched solution processed NiOx interlayers. Adv Energy Mater 2011;1:813–20.
[113] Chen CP, Chen YD, Chuang SC. High-performance and highly durable inverted organic photovoltaics embedding solution-processable vanadium oxides as an interfacial hole-transporting layer. Adv Mater 2011;23:3859–63.
[114] Kawano K, Ito N, Nishimori T, Sakai J. Open circuit voltage of stacked bulk heterojunction organic solar cells. Appl Phys Lett 2006;88, 073514/1–3.
[115] Hau SK, Yip HL, Baek NS, Zou J, O'Malley K, Jen AKY. Air-stable inverted flexible polymer solar cells using zinc oxide nanoparticles as an electron selective layer. Appl Phys Lett 2008;92, 253301/1–3.
[116] Sun YM, Seo JH, Takacs CJ, Seifter J, Heeger AJ. Inverted polymer solar cells integrated with a low-temperature-annealed sol–gel-derived ZnO film as an electron transport layer. Adv Mater 2011;23:1679–83.
[117] Seo HO, Park SY, Shim WH, Kim KD, Lee KH, Jo MY, Kim JH, Lee E, Kim DW, Kim YD, Lim DC. Ultrathin TiO_2 films on ZnO

electron-collecting layers of inverted organic solar cell. J Phys Chem C 2011;115:21517–20.
[118] Groenendaal LB, Jonas F, Freitag D, Pielartzik H, Reynolds JR. Poly(3,4-ethylenedioxythiophene) and its derivatives, past, present, and future. Adv Mater 2000;12:481–94.
[119] Tung VC, Kim JY, Cote LJ, Huang JX. Sticky interconnect for solution-processed tandem solar cells. J Am Chem Soc 2011;133:9262–5.
[120] Shrotriya V, Li G, Yao Y, Moriarty T, Emery K, Yang Y. Accurate measurement and characterization of organic solar cells. Adv Funt Mater 2006;16:2016–23.
[121] Li G, Shirotriya V, Huang J, Yang Y. Measurement issues of organic solar cells. SPIE Proc 2008;7052:70520E.
[122] Burdick J, Glatfelter T. Spectral response and I–V measurements of tandem amorphous-silicon alloy solar cells. Solar Cells 1986;18:301–14.
[123] Aramaki S. Solution-processible crystalline organic semiconductor for photovoltaic application. In: MRS Fall Meeting. 2011 [Abstr H8.6].
[124] Yang J, You JB, Chen CC, Hsu WC, tan HR, Zhang XW, Hong ZR, Yang Y. Plasmonic polymer tandem solar cell. ACS Nano 2011;5:6210–7.
[125] Xue JG, Uchida S, Rand BP, Forrest SR. Asymmetric tandem organic photovoltaic cells with hybrid planar-mixed molecular heterojunctions. Appl Phys Lett 2004;85:5757–9.
[126] Sun YM, Welch GC, Leong WL, Takacs CJ, Bazan GC, Heeger AJ. Solution-processed small-molecule solar cells with 6.7% efficiency. Nat Mater 2012;11:44–8.
[127] You JB, Chen CC, Hong ZR, Yoshimura K, Ohya K, Xu R, Ye SL, Gao J, Li G, Yang Y. 10.2% power conversion efficiency polymer tandem solar cells consisting of two identical sub-cells. Adv Mater 2013, http://dx.doi.org/10.1002/adma.201300964.
[128] Dou LT, Chang WH, Gao J, Chen CC, You JB, Yang Y. A selenium-substituted low-bandgap polymer with versatile photovoltaic applications. Adv Mater 2013;25:825–31.
[129] Li WW, Furlan A, Hendriks KH, Wienk MM, Janssen RAJ. Efficient tandem and triple-junction polymer solar cells. J Am Chem Soc 2013;135:5529–32.
[130] Walzer K, Maenning B, Pefiffer M, Leo K. Highly efficient organic devices based on electrically doped transport layers. Chem Rev 2007;107:1233–71.